TUBEDOWN IN THE REGULATION OF THE P53 TUMOR SUPPRESSOR PATHWAY

By © Cassandra Davidson

A Thesis submitted to the School of Graduate Studies

in partial fulfillment of the requirements for the degree of

Master of Science in Medicine

Division of Biomedical Sciences

Faculty of Medicine

Memorial University of Newfoundland

May 2019

St. John's Newfoundland and Labrador

ABSTRACT

Tubedown (TBDN) was initially discovered as a developmentally regulated protein, highly expressed during embryogenesis in neuroectodermal and mesenchymal lineages. TBDN is the regulatory subunit of the N^{α}-terminal acetyltransferase complex NatA, in conjunction with catalytic subunit Arrest-defective-1 protein (ARD1). In adulthood and aging, TBDN is involved in the regulation of retinal vascular permeability. It has been shown that TBDN is highly expressed in primitive bone tumors of mesenchymal and neuroectodermal origin, such as osteosarcoma (OS) and Ewing's sarcoma (EWS). Previous work in our lab suggests: TBDN is required for tumor cell growth via regulation of p53 tumor suppression; and, aged mice overexpressing TBDN under the inducible endothelial/mesenchymal *Tie2* promoter develop tumors in specific tissues. The focus of this study is to examine the role of TBDN in Ewing's sarcoma and during aging in mice, specifically in relation to p53 tumor suppression, in order to better understand the role of N^{α}-terminal acetyltransferases in cancer and aging.

The role of TBDN and ARD1 in the regulation of p53 levels and cell proliferation in Ewing's sarcoma cells *in vitro* was studied using an siRNA knockdown approach. The role of TBDN during aging was studied in a bi-transgenic *HHrtTAXK-TRE/HA-TBDN* mouse model overexpressing TBDN under the Dox-inducible endothelial/mesenchymal *Tie2* promoter.

Ewing's sarcoma cells knocked down for either TBDN or ARD1 expression showed upregulated p53 expression and reduced cell proliferation when compared to controls. The analysis of tumors collected from bi-transgenic *HHrtTAXK-TRE/HA-TBDN* aged mice overexpressing TBDN under the *Tie2* promoter showed overexpression of TBDN in the cells and blood vessels of the tumors. TBDN overexpression in mice during aging resulted in suppressed p53 expression in comparison to control mice. My results suggest that TBDN dysregulation of the tumor suppressor p53 could be involved in facilitating tumor formation.

ACKNOWLEDGEMENTS

I would like to thank my supervisors, Dr. Hélène Paradis and Dr. Robert Gendron for the guidance and support that they have provided throughout the completion of my Masters program. I would also like to thank my committee member, Dr. Kenneth Kao, for providing advice and valuable insight into my project.

In addition, I would like to thank present and past members of the Paradis/Gendron lab, Raahyma Ahmad, Karla Morrissey, Lidan Tao, and Michael Gardiner, for their assistance and support.

I would like to acknowledge funding support from the Memorial University Faculty of Medicine Dean's Fellowship as well as the Frederick Banting and Charles Best Canada Graduate Scholarship from CIHR.

CO-AUTHORSHIP STATEMENT

Co-authors:

Dr. Hélène Paradis (Faculty of Medicine, Memorial University)

Dr. Robert Gendron (Faculty of Medicine, Memorial University)

The siRNA transfections of the EWS-96 cell line and subsequent data analyses were conducted with the assistance of. Dr. Hélène Paradis (Faculty of Medicine, Memorial University). Upon completion of the siRNA transfection, I maintained the transfected cell cultures, analyzed transfection efficiencies, performed the *in vitro* cell growth assay, and prepared cell lysates. I also performed Western blots using these cell lysates.

The mouse model overexpressing TBDN under the control of the inducible endothelial/mesenchymal *Tie2* promoter was developed by Dr. Hélène Paradis. These mice were derived and the activity of the transgene characterized by Dr. Hélène Paradis (unpublished).

All mice were handled and sacrificed by Dr. Hélène Paradis and Dr. Robert Gendron (Faculty of Medicine, Memorial University). All mice tissues and abnormal tissue growths were collected by Dr. Hélène Paradis and Dr. Robert Gendron. Abnormal growths were analyzed and categorized by Dr. Hélène Paradis. I performed immunohistochemical analysis of the abnormal growths and corresponding control normal tissues. I also performed Western blots using tissue homogenate supernatants collected from mouse tissues. Assistance with the subsequent data analysis was provided by Dr. Hélène Paradis.

TABLE OF CONTENTS

LIST OF TABLES

LIST OF FIGURES

LIST OF ABBREVIATIONS

acetyl CoA	acetyl coenzyme A
Ala	alanine
AP	alkaline phosphatase
ARD1	Arrest-defective-1
ARD2	Arrest-defective-2
Asp	aspartic acid
BM-MSC	bone marrow mesenchymal stem cell
BMSC	bone marrow stromal cell
BSA	bovine serum albumin
CO_2	carbon dioxide
DMEM	Dulbecco's modified eagle medium
DNA	deoxyribonucleic acid
EDTA	ethylenediaminetetraacetic acid
EWS	Ewing's sarcoma
EWSR1	Ewing's sarcoma RNA binding protein 1, Ewing's sarcoma breakpoint region 1
EWS-96	Ewing's sarcoma cell line
FBS	fetal bovine serum

FLI1	Fli-1 proto-oncogene, ETS transcription factor
GFP	green fluorescent protein
Glu	glutamic acid
Gly	glycine
H&E	hematoxylin and eosin staining
HA-tag	human influenza hemagglutinin tag
HRP	horseradish peroxidase
IEM	embryonic endothelial cell line
Lys	lysine
MDM2	murine double minute 2
Met	methionine
ms	millisecond
NatA	N^{α}-terminal acetyltransferase A
OS	Osteosarcoma
Osx	Osterix
PBS	phosphate buffered saline
PCNA	proliferating cell nuclear antigen
RNA	ribonucleic acid

Runx2	Runt-related transcription factor 2
SDS-PAGE	sodium dodecyl sulfate polyacrylamide gel electrophoresis
Ser	serine
siRNA	short-interfering ribonucleic acid
Src	proto-oncogene non-receptor tyrosine kinase
TBDN	Tubedown
TESPA	3-triethoxysilylpropylamine
Thr	threonine
Trp	tryptophan
V	volts
Val	valine
WWOX	WW domain-containing oxidoreductase

Chapter 1 Introduction

1.1 N^{α}-terminal acetyltransferase A (NatA)

Acetylation is a post-translation modification carried out by the reversible and opposing actions of acetyltransferases and deacetylases (Brock 2010). The acetylation of protein substrates ultimately modulates their stability and activity (Brock 2010). Specifically, N^{α}-terminal acetyltransferases facilitate the addition of acetyl groups to the N-termini of their substrate polypeptides.

NatA is an N^{α}-terminal acetyltransferase with thousands of potential substrates and is known to play a role in cell growth and differentiation (Arnesen et al. 2009, Gromyko et al. 2010). The NatA complex is made up of a catalytic subunit and a regulatory subunit. The catalytic subunit enzymatically facilitates the co-translational acetylation of the substrate at its N-terminus, with acetyl coenzyme A (acetyl CoA) acting as the acetyl group donor. This acetylation occurs after the cleavage of the initiating methionine (Met) residue by methionine aminopeptidase, and only on substrate polypeptides with alanine (Ala), serine (Ser), threonine (Thr), glycine (Gly), or valine (Val) N-terminal residues (Gromyko et al. 2010) (Figure 1A). In the NatA complex, the catalytic subunit is Arrest-defective-1 (ARD1, also referred to as Naa10) or Arrest-defective-2 (ARD2, also referred to as Naa11; 81% identity between the two isoforms ARD1/Naa10 and ARD2/Naa11) (Arnesen et al. 2009, Gendron et al. 2000, Gromyko et al. 2010). The acetyltransferase activity of the NatA complex is modulated by its regulatory subunit. In the NatA complex, the regulatory subunit is Naa16 or Tubedown (TBDN, also referred to as Naa15, Nat1, or Narg1; 70% identity between the two isoforms TBDN/Naa15 and Naa16) (Arnesen et al. 2009, Gendron et al. 2000, Gromyko et al. 2010).

The NatA complex, made up of ARD1 and TBDN subunits, has been shown to be important in the maintenance of normal cell viability in multiple human cell lines (Arnesen et al. 2009). Since it is known that acetyltransferases play a role in modulating the activity of a number of factors responsible for normal cell growth and differentiation, including cyclin D1, Rb/E2F, and p27/Kip1, it has been proposed that acetyltransferases may be effective potential targets for cancer treatments (Gromyko et al. 2010).

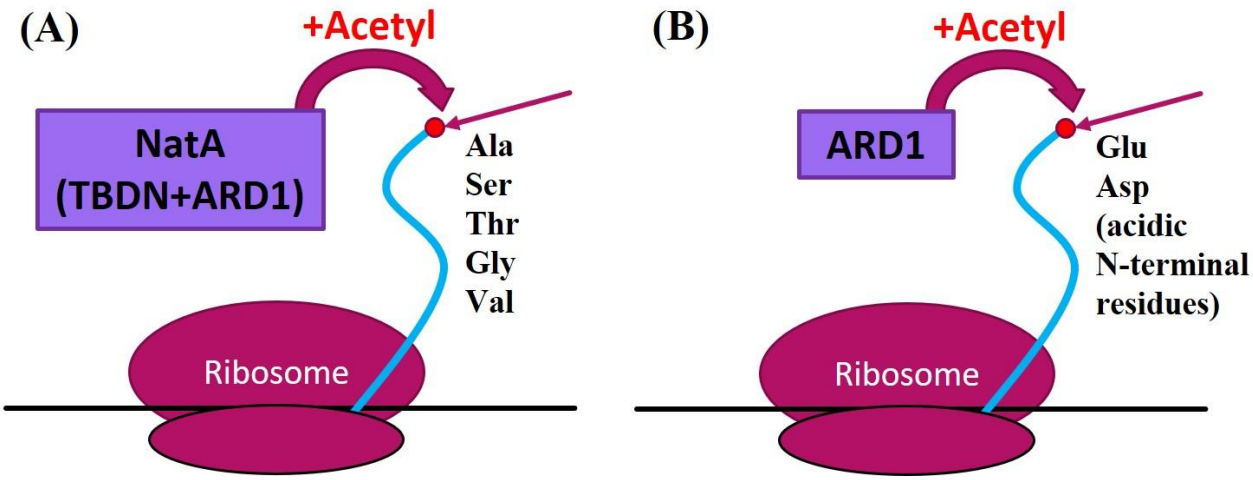

Figure 1. Schematic diagram showing the catalytic activity of N^{α}-terminal acetyltransferase NatA.

(A) NatA is made up of two subunits, TBDN and ARD1. NatA cotranslationally acetylates its substrate polypeptide chain at alanine, serine, threonine, glycine, or valine residues at the N-terminus.

(B) ARD1, the catalytic subunit of the NatA complex, shows acetyltransferase activity independent of regulatory subunit TBDN. ARD1 cotranslationally acetylates its substrate polypeptide chain at glutamic acid or aspartic acid residues at the N-terminus.

1.1.1 NatA catalytic subunit, ARD1

Arrest-defective-1 protein (ARD1; also referred to as Naa10) is the catalytic subunit of the NatA complex. ARD1 contains a loop structure; this structure suggests that certain substrate residues are blocked from entering the active site of ARD1 for acetylation in its 'closed' loop state (Magin et al. 2016). The binding of ARD1 with NatA regulatory subunit TBDN induces a conformational change in the structure of ARD1; this changes the characteristic 'closed' loop structure, opening its active site and allowing it to acetylate NatA substrate polypeptide chains with alanine (Ala), serine (Ser), threonine (Thr), glycine (Gly), or valine (Val) N-termini residues (Liszczak et al. 2013) (Figure 1A). Independently of TBDN, ARD1 is able to acetylate substrate polypeptides at N-terminal acidic residues, aspartic acid (Asp) or glutamic acid (Glu) (Magin et al. 2016) (Figure 1B). Also, ARD1 is able to acetylate internal lysine residues of specific substrates upon its hydroxylation at tryptophan residue Trp-38 (Kang et al. 2018). The hydroxylation of ARD1 occurs in an oxygen-dependent manner, meaning that the acetylation of internal lysine residues by ARD1 is also oxygen dependent (Kang et al. 2018).

In humans, it is known that ARD1 mutations can cause developmental defects; these defects can affect the cardiac, skeletal, and ocular systems, and can also result in behavioural abnormalities, developmental delay, and muscular hypotonia (Saunier et al. 2016). In mice, ARD1 is widely expressed and negatively regulates early postnatal osteogenesis. In ARD1 knockout mice, there were a number of severe developmental defects observed including bone abnormalities, developmental defects, and growth retardation (Vo et al. 2018). This suggests that human ARD1 mutants may have dominant inhibitory effects.

ARD1 knockout mice show denser and more extended bone development relative to their littermates (Vo et al. 2018). It is known that ARD1 is involved in bone development and

remodelling (Yoon et al. 2014). ARD1 is stabilized by Runt-related transcription factor 2 (Runx2) in osteoblasts during bone differentiation (Yoon et al. 2014). Upon its stabilization, ARD1 as the catalytic subunit of the NatA complex acetylates Runx2 at internal lysine residue Lys-225; this acetylation inhibits Runx2 enzymatic activity. In turn, ARD1 controls Runx2 bone differentiation by inhibiting its activation of osteoblast differentiation genes in a feedback mechanism (Yoon et al. 2014).

The mechanistic role of ARD1 in cancer has not been clearly elucidated; ARD1 has been shown to function as both a tumor suppressor and an oncoprotein in different types of cancer cells (Kalvik and Arnesen 2013). ARD1 is known to show pro-proliferative and anti-apoptotic activity in certain types of cancer cells (Kalvik and Arnesen 2013). ARD1 is known to be overexpressed in lung, colorectal, bladder, and cervical cancers, and in the context of these cancers has been linked to more aggressive tumor states and poorer patient outcomes (Kalvik and Arnesen 2013, Yu et al. 2009). Deregulated human ARD1 or NatA expression is linked to tumor development or progression (Myklebust et al. 2015). It has been shown that the knockdown of ARD1 expression in cells reduces cell proliferation, enforcing the role of ARD1 in the promotion of cell proliferation and cancer cell survival (Kalvik and Arnesen 2013).

In other cancer cell types, ARD1 has also been shown to have anti-proliferative and pro-apoptotic activity. Specifically, a high level of ARD1 expression in breast cancer is linked to smaller tumor size, lower incidence of lymph node metastases, and better patient survival (Kuo et al. 2010). The downregulation of ARD1 expression promotes both tumor progression and cancer cell migration by disruption of the migratory complex PIX-GIT-Paxillin in lung, breast, ovarian, and gastric cancer cells (Hua et al. 2011, Kalvik and Arnesen 2013). ARD1 can demonstrate tumor suppressive properties, mainly linked to its role in the inhibition of cell

motility and promotion of autophagy as shown in lung, breast, ovarian, and gastric cancer cells (Kalvik and Arnesen 2013). The specific role of ARD1 in cancer cells is dependent upon the type of tumor and the tissue in which it originates.

1.2 Tubedown (TBDN)

Tubedown (TBDN; also referred to as Naa15, Narg1, NATH) is the regulatory subunit of the NatA complex. TBDN anchors ARD1, the catalytic subunit of NatA, to the ribosome and modulates the enzymatic acetyltransferase activity of the NatA complex (Liszczak et al. 2013). The binding of TBDN to ARD1 induces a conformational change, exposing its active site and allowing the complex to acetylate NatA substrates (Liszczak et al. 2013).

TBDN was discovered as a developmentally regulated protein, highly expressed and tightly regulated during embryogenesis (Gendron et al. 2000). The Paradis/Gendron lab group determined that TBDN is a subunit of the NatA acetyltransferase complex. It is known that TBDN is involved in: embryogenesis and development; the regulation of retinal vascular permeability; and certain cancers (Gendron et al. 2000, Gendron et al. 2001, Gendron et al. 2010, Paradis et al. 2002, Kalvik and Arnesen 2013**,** Martin et al. 2007, Starheim and Gromyko et al. 2009, Sugiura et al. 2003).

1.2.1 Tubedown in development

The expression of TBDN is highly regulated during embryogenesis. During embryogenesis, there are three distinct lineages that give rise to all tissue types in the adult: ectoderm, mesoderm, and endoderm. Mesoderm gives rise to a number of tissue lineages, including connective tissues, endothelium, neural tissues, adipose tissues, blood and lymphatic tissues, among others (Dyer and Patterson 2010, Harvey and Oliver 2004). TBDN is known to

be highly expressed in a number of mesodermally-derived tissues during embryogenesis and development. Particularly high levels of TBDN expression are seen in hematopoietic, vascular, bone, and eye lineages during embryogenesis (Gendron et al. 2000). Specifically, TBDN expression is tightly regulated during the differentiation of vascular and neuronal tissues (Gendron et al. 2001, Sugiura et al. 2003). TBDN is also highly expressed and tightly regulated in other embryonic tissues during development. In mice, it has been observed that TBDN is highly expressed in neuronal cells during brain development, as the cells divide and migrate; TBDN is then subsequently downregulated during neuronal maturation (Sugiura et al. 2003). A role for TBDN in the inhibition of blood vessel formation has also been suggested, as it has been shown that TBDN is downregulated during capillary-like formation of IEM embryonic endothelial cells (Gendron et al. 2000, Paradis et al. 2002).

1.2.2 Tubedown in adulthood

In the adult, TBDN expression is undetectable in most tissues. High levels of TBDN expression in the adult are isolated to blood vessels of regressing ovarian follicles, the ocular endothelium, and the choroid plexus endothelium, as well as the atrial endocardium, bone marrow, and eyes (Gendron et al. 2000, Gendron et al. 2001, Paradis et al. 2002).

The Paradis/Gendron lab has characterized TBDN as a novel homeostatic factor shown to be involved in blood vessel growth and homeostasis (Gendron et al. 2000, Gendron et al. 2001, Paradis et al. 2002). During adulthood, it is known that TBDN regulates retinal blood vessel permeability and Src tyrosine kinase-mediated cell permeability (Ho et al. 2015). It is known that TBDN levels decrease during aging, as demonstrated in the retinal and choroidal vasculature (Gendron et al. 2010).

1.2.3 Tubedown in cancer

The expression of TBDN has been studied in the context of multiple cancers, including papillary thyroid carcinoma, gastric cancers, and certain childhood cancers – namely, neuroblastoma, osteosarcoma (OS), and Ewing's sarcoma (EWS) (Martin et al. 2007, Starheim and Gromyko et al. 2009, Kalvik and Arnesen 2013; Dr. H. Paradis, personal communication). TBDN has been shown to be highly expressed in papillary thyroid carcinoma, neuroblastoma, OS, and EWS (Martin et al. 2007, Kalvik and Arnesen 2013; Dr. H. Paradis, personal communication). In the context of neuroblastoma, high TBDN expression correlates with a less favourable tumor histology, less differentiated tumors, and a more advanced disease stage (Martin et al. 2007).

TBDN is also highly expressed in primitive bone tumors of mesenchymal and neuroectodermal origin, including OS and EWS (Dr. H. Paradis, personal communication). Recent unpublished data collected in the Paradis/Gendron lab suggest that TBDN is necessary for regulation of the growth of EWS cells and tumor xenografts in mice, and the regulation of p53 tumor suppression (Dr. H. Paradis, personal communication).

1.3 The p53 pathway

1.3.1 p53 function

The tumor suppressor p53 is often referred to as the 'guardian of the genome.' In acting as a transcription factor, p53 is involved in the regulation of cell cycle arrest, apoptosis, DNA repair, and senescence (Barone et al. 2014, Brooks and Gu 2011, Dai and Gu 2010, Meek 2015, Reed and Quelle 2015). In the normal mature cell, p53 is maintained at low levels and is only

activated during cell stress events in order to exert its tumor suppressive functions (Barone et al. 2014, Brooks and Gu 2011, Reed and Quelle 2015, Takiar et al. 2016).

p53 expression is tightly regulated during embryogenesis and development. During organ development in embryogenesis, pronounced p53 expression is seen in the differentiation of brain, liver, lung, thymus, intestines, salivary glands, and kidneys (Nostrand et al. 2017). p53 is also referred to as the 'safeguard of differentiation' due to its involvement in the development and the ongoing maintenance of numerous tissue types and organs.

However, there is evidence to suggest that p53 may be dispensable for normal development (Nostrand et al. 2017). p53-deficient mice appear normal at birth, with p63 and p73 gene products demonstrating functionally redundant roles and compensating for the lack of p53 expression during embryogenesis (Donehower et al. 1992, Liu and Li 2010, Nostrand et al. 2017). This functional redundancy is expected, as p53 family members including p63 and p73 are highly conserved structurally (Nostrand et al. 2017).

p53 is a negative regulator of osteoblastogenesis. p53 inhibits osteoblast differentiation and proliferation, while enhancing osteoblast apoptosis (Del Mare et al. 2016, Komori 2016). The mechanism of the repressive effects of p53 on osteoblast differentiation, bone development, and bone remodelling is unknown (Artigas et al. 2017, Komori 2016). Bone formation is coregulated by p53 and WW domain-containing oxidoreductase (WWOX) through the control of osteoblast differentiation (Del Mare et al. 2016). In mice with a mutation or deletion of normal WWOX and p53, the development of osteosarcoma is accelerated (Del Mare et al. 2016).

p53 deficiency is linked to increased bone formation; this is due to the enhanced proliferation and differentiation of mesenchymal stem cells and osteoprogenitor cells brought on

by the absence of p53 (Liu and Li 2010). It is known that p53 is involved in the differentiation of osteoblasts via the regulation of the transcription factors Runt-related transcription factor 2 (Runx2) and Osterix (Osx); specifically, p53 inhibits Runx2 and thereby suppresses osteoblast differentiation (Liu and Li 2010, Rubio et al. 2013). As they age, p53-deficient mice demonstrate an osteosclerotic phenotype, with modest increases in bone mineral density and bone volume, when compared to their control littermates (Liu and Li 2010). p53-deficient mice also have denser skeletons and specific skeletal deformities, including upper incisor fusion, and craniofacial and limb malformations (Artigas et al. 2017, Liu and Li 2010). In addition to these skeletal abnormalities, the bone marrow mesenchymal stem cells (BM-MSCs) of p53-deficient mice have an increased tendency to undergo differentiation to osteoblasts (Artigas et al. 2017). The bone marrow stromal cells (BMSCs) of p53-deficient mice also undergo enhanced osteogenic differentiation (He et al. 2015). p53-deficient mice experience a number of bone and skeletal abnormalities during growth and into adulthood, despite their normal appearance at birth and normal embryogenesis. The p53 family members cannot successfully compensate for the functionality of p53 specifically during growth and aging, as they do during embryogenesis.

1.3.2 p53 regulation

The tumor suppressor p53 is often referred to as the 'guardian of the genome' as it is involved in the regulation of cell cycle arrest, apoptosis, DNA repair, and senescence (Barone et al. 2014, Brooks and Gu 2011, Dai and Gu 2010, Meek 2015, Reed and Quelle 2015). Normally, p53 is maintained at low levels in the cell by a negative feedback loop with murine double minute 2 (MDM2) (Barone et al. 2014, Brooks and Gu 2011, Reed and Quelle 2015, Takiar et al. 2016). MDM2 is an E3 ubiquitin ligase which controls p53 activity and stability via an autoregulatory negative feedback loop (Barone et al. 2014, Reed and Quelle 2015, Takiar et al.

2016). MDM2 is able to negatively regulate p53 by blocking p53 transactivation, recruiting p53 corepressors, and stimulating the degradation of p53 (Barone et al. 2014). Under 'normal' unstressed cellular conditions, MDM2 applies its E3 ubiquitin ligase activity and marks p53 for ubiquitination at the proteasome (Barone et al. 2014). When the cell is under stress, the p53 protein is stabilized and will accumulate in the cell.

p53 is stabilized and activated by cellular stress events, including DNA damage, telomere erosion, and hypoxia (Barone et al. 2014, Brooks and Gu 2011, Dai and Gu 2010). This stabilization of p53 due to cell stress will result in the rapid accumulation of p53 protein in the cell. Upon activation, p53 exerts its tumor suppressive activity by forming an active tetrameric structure and acting as a transcription factor to activate the expression of specific genes (Brooks and Gu 2011, Reed and Quelle 2015, Takiar et al. 2016).

Post-translational modifications – including acetylations, phosphorylations, ubiquitinations, and methylations – applied to p53 can modulate its protein stability and activity within the cell (Brooks and Gu 2011, Reed and Quelle 2015). In general, acetylations are a set of reversible post-translational modifications executed by the reversible and opposing actions of acetyltransferases and deacetylases, which modulate the stability and activity of protein substrates (Brock 2010).

Specifically, p53 acetylation occurs in response to DNA damage and genotoxic stress at specific lysine (Lys) residues (Brooks and Gu 2011). The acetylation of p53 leads to many effects which result in the stabilization and accumulation of p53 in the cell. The effects of p53 lysine acetylation include: the exclusion of p53 ubiquitination; the inhibition of complex formation with MDM2 at target gene promoters; the alteration of p53's DNA binding affinity; and the recruitment of cofactors to stimulate p53 transcriptional activity (Dai and Gu 2010, Reed

and Quelle 2015, Tang et al. 2008). p53 lysine acetylation blocks the recruitment of MDM2 and results in the accumulation and activation of p53 in the cell (Tang et al. 2008). The addition of acetyl groups at specific lysine residues in the p53 protein structure – Lys-120, Lys-164, and the C-terminal DNA-binding domain, in particular – strengthen its ability to specifically bind both *its protein substrates and target DNA sequences (Reed and Quelle 2015).

When the normal lysine acetylation pattern of p53 is disrupted, this inhibits the normal functions of p53 (Reed and Quelle 2015). Alterations to normal p53 acetylation will result in the loss of normal p53 functions – including the regulation of cell cycle arrest, senescence, and apoptosis.

1.3.3 p53 dysregulation in aging and cancer

p53-deficient mice undergo normal embryogenesis due to the functional redundancies of p53 family members p63 and p73, and subsequently appear normal at birth (Donehower et al. 1992, Liu and Li 2010, Nostrand et al. 2017). However, p53-deficient mice demonstrate some phenotypic differences as they mature. These mice show increased sensitivity to carcinogenic agents and are highly cancer prone with aging. By age 5 to 7 months, p53-deficient mice (homozygotes) show increased incidence of a range of tumor types, mainly lymphomas (Donehower et al. 1992, Jacks et al. 1994, Liu and Li 2010). Mouse heterozygous for p53 deficiency showed mainly sarcomas (ie. osteosarcoma, fibrosarcoma, hemangiosarcoma, lyomyosarcoma), lung adenocarcinomas, and lymphomas (Jacks et al. 1994, Liu and Li 2010). As a result of increased tumor incidence, p53-deficient mice have a shorter lifespan than their wildtype control littermates.

It is known that p53 expression and activation is involved in the cellular aging process (Rufini et al. 2013). During aging there is an increase in oxidative damage and DNA damage present in cells; this activates p53 and results in the presence of increased p53 protein levels in the tissues of aging mice (Rufini et al. 2013).

The tumor suppressor p53 itself and components of the p53 pathway are often mutated in human cancers. It is known that p53 itself is mutated or lost in 55% of tumors, while p53 signalling targets and/or regulators are mutated or deregulated in the remaining percentage of tumors (Barone et al. 2014, Nostrand et al. 2017, Reed and Quelle 2015).

Mutations in the p53 pathway or its regulators will result in tumor progression (Barone et al. 2014, Takiar et al. 2016). Cells with mutations affecting the normal tumor suppressive functions of p53 are predisposed to incur permanent damage by cell stress events; this increases the likelihood of tumor development (Reed and Quelle 2015). p53 mutations, often missense mutations in the DNA binding domain, play a role in tumorigenesis by interrupting the tumor suppressive functions of p53 and triggering its oncogenic functions (Dai and Gu 2010). The oncogenic functions of mutated p53 include: providing a selective growth advantage for cells with the p53 mutations; transactivating new target genes responsive to the mutant form of p53; and interacting with inappropriate cellular proteins (Dai and Gu 2010). Also, the acetyltransferases responsible for performing post-translational modifications to p53 are often mutated in cancers, resulting in the inhibition of the normal tumor suppressive functions of p53 (Reed and Quelle 2015). This can interrupt p53 tumor suppressive functions by preventing the acetylation of key lysine residues on the p53 protein polypeptide chain, preventing the activation of its transcriptional activity.

1.4 Ewing's sarcoma (EWS)

Ewing's sarcoma (EWS) is a heterogeneous and aggressive tumor of the bone and soft tissue (Arndt and Crist 1999, Biswas and Bakhshi 2016, Fizazi et al. 1998, Palumbo and Zwerdling 1999, Pishas and Lessnick 2016). It is the second most common primary malignant bone tumor, with peak incidence occurring in adolescence (Biswas and Bakhshi 2016). Morphologically, EWS tumors are described as small round cell neoplasms of neuroectodermal origin (Amann et al. 1999, Barone et al. 2014, Kim and Park 2016, West 2000). TBDN has been shown to be highly expressed in the Ewing's sarcoma EWS-96 cell line (Dr. H. Paradis, personal communication).

Genetically, most Ewing's sarcoma tumors show either of two chromosomal translocations: between chromosomes 11 and 22: t(11;22)(q24;q12); or between chromosomes 21 and 22 t(21;22)(q22;q12) (de Alava and Gerald 2000, Kim and Park 2016). *EWSR1* is located on chromosome 22q12, and *FLI1* is located on chromosome 11q24 (Kim and Park 2016). The most common mutations associated with EWS tumors are *EWSR1* gene rearrangement and *EWSR1 + FL1* gene chromosomal fusion (Kim and Park 2016, Lin et al. 2010, Pishas and Lessnick 2016, Yu et al. 2016). These translocations involve the region of the 5' end of the Ewing's sarcoma (*EWS*) gene fusing with the 3' end of an ETS family transcription factor, either *FLI-1* or *ERG* (Arndt and Crist 1999, de Alava and Gerald 2000, Palumbo and Zwerdling 1999).

EWS is associated with a number of mutations in some readily-targetable signal transduction pathways (Pishas and Lessnick 2016). p53 mutations are fairly rare, with approximately 90% of EWS tumors still possessing wildtype p53 (Barone et al. 2014). *EWSR1* gene rearrangement has been reported to occur in approximately 90% of EWS cases (Kim and Park 2016). The EWS/ETS fusion proteins resulting from the commonly-associated Ewing's

sarcoma mutations show DNA binding activity and are oncogenic (Arndt and Crist 1999, de Alava and Gerald 2000, Palumbo and Zwerdling 1999). The DNA binding activity of EWS/ETS fusion proteins is known to regulate the expression of specific genes involved in development, proliferation, apoptosis, and oncogenesis (de Alava and Gerald 2000, West 2000). The actual mechanism by which EWS/ETS fusion proteins, specifically EWS/FLI-1 proteins, impact the growth of Ewing's sarcoma tumors has not been determined (de Alava and Gerald 2000). Further, it is known that EWS/FLI-1 fusion proteins are not able to transform all cells, with some requiring input from other factors (de Alava and Gerald 2000).

Treatment options for Ewing's sarcoma are limited and patients show variable rates of survival. Ewing's sarcoma patients have a survival rate of 20-30%, while patients with localized disease show 70-80% survival (Fergurson and Turner 2018). The current treatment for Ewing's sarcoma involves cytotoxic drug chemotherapy followed by radiation and surgery (Arndt and Crist 1999, Biswas and Bakhshi 2016, Palumbo and Zwerdling 1999, Yu et al. 2016). These treatments present a risk of relapse, in both metastatic and localized disease (Ferguson and Turner 2018, Fizazi et al. 1998, West 2000). Available treatments for Ewing's sarcoma need to be improved in order to increase survival rates.

New treatment strategies for Ewing's sarcoma targeting the signalling pathways involved in regulating the growth of tumor cells could increase survival rates. Recent unpublished data collected in the Paradis/Gendron lab suggest that the N^{α}-terminal acetyltransferase subunit Tubedown (TBDN) regulates the growth, differentiation processes, and p53-mediated tumor suppression of Ewing's sarcoma. TBDN may offer a new potential target for Ewing's sarcoma treatments.

1.5 Rationale behind current study

Tubedown (TBDN) was originally discovered as a developmentally regulated protein. TBDN is known to be tightly regulated and highly expressed during embryogenesis. Specifically, TBDN is highly expressed in neuroectodermal and mesenchymal lineages during development. We also know that TBDN expression decreases during normal aging in tissues of the adult, as demonstrated by the Paradis/Gendron lab in the retinal vasculature.

TBDN has been shown to be highly expressed in certain childhood cancers, including neuroblastoma, osteosarcoma, and Ewing's sarcoma (EWS). Previous work by the Paradis/Gendron lab suggested that TBDN is necessary for the growth of EWS cells *in vitro* and tumor xenografts in mice through regulation of the tumor suppressor p53. Based on this, TBDN may be a good candidate for developing a targeted therapy in the treatment of EWS.

In the Paradis/Gendron lab, the role of TBDN during aging is studied in a bi-transgenic mouse model overexpressing TBDN under the control of the inducible endothelial/mesenchymal *Tie2* promoter (*HHrtTAXK-TRE/HA-TBDN*) developed by Dr. Hélène Paradis (Faculty of Medicine, Memorial University) (Figure 2). Doxycycline (Dox) administered in the diet was used to achieve induction of the *Tie2* promoter, and subsequent overexpression of TBDN specifically in endothelial and mesenchymal tissues (Figure 2). These mice were derived and the activity of the transgene characterized by Dr. Hélène Paradis (unpublished).

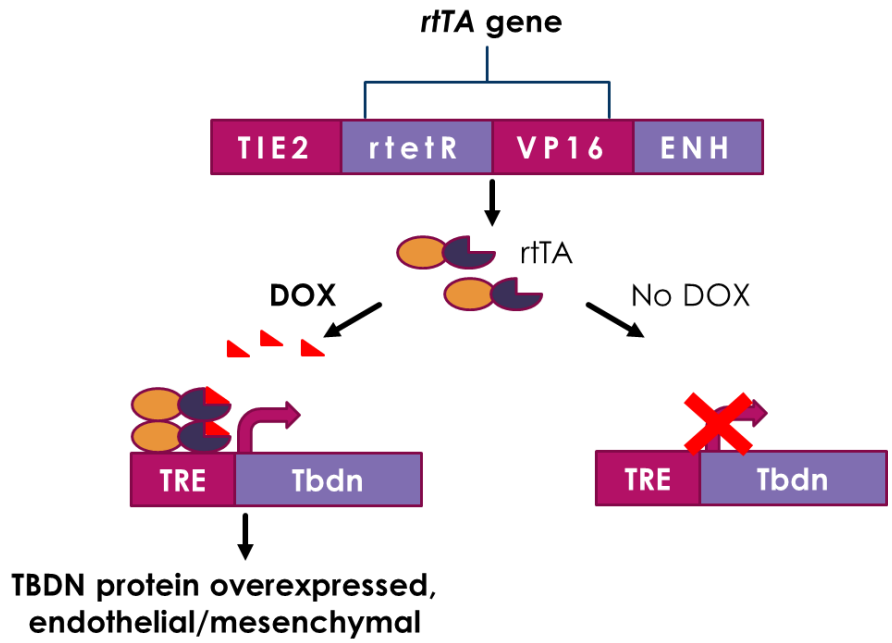

Figure 2. Schematic diagram showing the overexpression of Tubedown in the bi-transgenic *Tie2/rtTA/Enh-TRE/HA-TBDN* mouse model, under the control of the inducible endothelial/mesenchymal *Tie2* promoter.

The *Tie2* endothelial/mesenchymal promoter (TIE2) regulates the expression of the rtTA protein (Wall et al. 2004). In the presence of doxycycline (DOX) in the diet, rtTA binds and activates the tetracycline response element promoter (TRE); this directs the expression of the downstream *Tbdn* gene (Tbdn) and results in the overexpression of Tubedown in endothelial and mesenchymal tissues. In the absence of DOX, rtTA does not bind the TRE promoter and TBDN is not overexpressed. TIE2, inducible endothelial/mesenchymal promoter; *rtTA* gene = rtetR + VP16, reverse tetracycline-controlled transcriptional transactivator gene; ENH, enhancer; DOX, doxycycline; TRE, tetracycline response element promoter; Tbdn, Tubedown gene.

These mice were derived and the expression and activity of the transgene characterized by Dr. Hélène Paradis (Faculty of Medicine, Memorial University; unpublished). The Paradis/Gendron

lab has derived three genotypes of mice: bi-transgenic mice *Tie2/rtTA/Enh-TRE/HA-TBDN* (ie. transgenic for Tubedown overexpression; referred to as *HHrtTAXK-TRE/HA-TBDN* in the Paradis/Gendron lab); and our control transgenics, *Tie2/rtTA/Enh* (referred to as *HHrtTAXK* in the Paradis/Gendron lab) and *TRE/HA-TBDN*. The expression and activity of the transgene was confirmed by Dr. Hélène Paradis (Dr. H. Paradis, personal communication); tissues were also provided by Dr. Hélène Paradis for this study.

Abnormal tissue growths collected from the mouse cohort (*HHrtTAXK-TRE/HA-TBDN*, *HHrtTAXK*, and *TRE/HA-TBDN*) upon sacrifice by Dr. Hélène Paradis and Dr. Robert Gendron were analyzed and categorized by Dr. Hélène Paradis (Faculty of Medicine, Memorial University). No abnormal growths have been found so far in the *TRE/HA-TBDN* control aged mice. No abnormal growths were observed in middle aged mice; abnormal tissue growths were only seen in aged mice greater than 16 months old (Dr. H. Paradis, personal communication).

The control aged mice (*HHrtTAXK* control aged mice) showed lower incidence of abnormal growths than the Dox-induced aged mice transgenic for TBDN overexpression. Incidence of abnormal growths in the non-induced aged mice transgenic for TBDN overexpression is being assessed by Dr. Hélène Paradis and Dr. Robert Gendron. Notably, abnormal growths were only found in the lung tissue of the *HHrtTAXK* control aged mice and non-induced bitransgenic *HHrtTAXK-TRE/HA-TBDN* aged mice. In the Dox-induced aged mice transgenic for TBDN overexpression, abnormal growths were collected from 8 different tissues, including lung, equating to 23.8% incidence (Dr. H. Paradis, personal communication).

My hypothesis is that TBDN expression regulates the p53 tumor suppressor pathway in cancer. We predict that TBDN is involved in modulating the NatA acetylation of a p53 pathway regulator, and therefore regulates the levels of p53 expressed in the cell.

1.5.1 Research objectives

Aim 1: Examine the impact of TBDN knockdown on the p53 pathway in Ewing's sarcoma EWS-96 cells.

Aim 2: Examine the impact of TBDN overexpression in the vasculature (endothelium) and mesenchymal lineages in mice on the p53 pathway during aging.

I aimed to study the impact of TBDN knockdown and overexpression on the p53 tumor suppression pathway. I am looking at the role of TBDN in the p53 tumor suppressor pathway in Ewing's sarcoma *in vitro*. I also want to determine the impact of TBDN overexpression in the vasculature (endothelial tissues) and mesenchymal tissues on the p53 pathway during aging in mice.

Overall, the goal of the research is to better understand the role of N^{α}-terminal acetyltransferases in cancer and aging in order to identify better targets for the design of new treatments for cancer.

Chapter 2 Materials and Methods

2.1 Cell culture

EWS-96 Ewing's sarcoma cell line (isolated and characterized by Dr. Theodore Zwerdling, Miller Children's Hospital, Long Beach, CA) was cultured in low glucose Dulbecco's modified eagle medium (DMEM) supplemented with 10% fetal bovine serum (FBS, heat inactivated) and 2 mM glutamine (Q). All cells were cultured at 37˚C in a 10% carbon dioxide (CO_2) atmosphere. Cells were cultured in 100mm, 60mm, and 35mm plates as necessary. $12x10^6$ cells are present in a 100% confluent 100mm plate of EWS-96.

The cells were quantified by trypsinizing the cells to detach them from the plate, followed by manual counting with a hemacytometer. Trypsin-EDTA (0.25%) was used as a cell dissociation agent for splitting and replating cells, with an 8-10 minute incubation in 0.25% Trypsin-EDTA at 37˚C in a 10% CO_2 atmosphere. Viable cells were counted using Trypan blue dye exclusion (1x, used at 0.185 mg/mL).

2.2 Antibodies

Mouse monoclonal anti-ARD1 (A10; sc-373920), anti-NARG1 (sc-81643), and anti-p53 (Pab240; sc-99) antibodies were obtained from Santa Cruz Biotechnology (Santa Cruz, CA). Loading controls used for Western blot analysis included: rabbit polyclonal anti-STAT3 (C-20; sc-482) and mouse monoclonal anti-actin β/γ antibodies, obtained from Santa Cruz Biotechnology (C-4; sc-47778; Santa Cruz, CA); and mouse monoclonal anti-α-tubulin (T-9026), obtained from Sigma (St. Louis, MO). STAT3 was used as a loading control for cell lysates analyzed by Western blot in our lab, since it is known that STAT3 is highly expressed in our EWS-96 Ewing's sarcoma cells (Dr. H. Paradis and Dr. R. Gendron, personal

communication). Actin or Tubulin were used as loading controls for tissue homogenates analyzed by Western blot in our lab.

We used horseradish peroxidase (HRP) conjugated anti-mouse IgG and anti-rabbit IgG secondary antibodies for analysis by Western blot (Promega, Madison, WI). Alkaline phosphatase (AP) conjugated anti-mouse IgG and anti-rabbit IgG (Promega, Madison, WI) and anti-mouse IgG2a (Vector Laboratories, Inc., Burlingame, CA) secondary antibodies were used in immunohistochemistry.

2.3 siRNA transfection

I conducted a human BLAST search for all siRNAs used to gauge off-target effects in the EWS-96 human cell line. No significant homology of any siRNA used was found; therefore, no off-target effects are expected with any siRNA used in my transient siRNA knockdown approach. *TBDN* siRNAs and the scrambled control siRNA were purchased from Dharmacon RNA technologies (Fisher Scientific, Ottawa, ON). *ARD1* siRNAs and the scrambled control siRNA were purchased from ThermoScientific (Burlington, ON).

Multiple *TBDN* siRNAs were tested. TBDN was knocked down using duplex siRNA corresponding to *TBDN* cDNA within the coding region (5'-GGGACCUUUCCUUACUACAUU-3'), (5'-GAAGGCUGCCGUUAAACUUUU-'3'), or (5'-UGCGAGAUCUUGAGGGUUAUU-3'). Scrambled control siRNAs (5'-UCAUAUCGAUUCGUGCCACUU-3'), (5'-GAUCCGUUCAUCGUCACUAUU-3'), or (5'-ACUUAUCGAUUCGGUCCACUU-3') were used as a control. *TBDN* siRNA and its control scrambled siRNA were tested at concentrations of 5 nM, 10 nM, and 20 nM.

ARD1 was knocked down using duplex siRNA corresponding to *ARD1* cDNA within the coding region (5'-CCAGAUGAAAUACUACUUCUU-3') and scrambled control siRNA (5'-ACUAACGUUACGUACAUCAUU-3'). *ARD1* siRNA and its control scrambled siRNA were tested at concentrations of 5 nM, 10 nM, and 20 nM.

My siRNA transfection protocol was adopted from the protocol presented in Ho et al. (2015). The transfection was performed using the Neon Transfection System (Life Technologies Inc., Burlington, ON) following the protocols specified by the manufacturer. Transfection parameters used were: 2 pulses at 1300 volts (V), with a 20 millisecond (ms) pulse width. Transfection efficiencies were determined by cotransfecting the cells with the green fluorescent protein (GFP) plasmid pMax GFP (Lonza, Cologne, Germany). Fluorescence microscopy was used to evaluate transfection efficiency with the plasmid pMax GFP at 24 hours post-transfection. Images were obtained at 10x magnification after focussing the microscope with the non-transfected control plate. Media was changed and cells were allowed to grow for an additional 24 hours. Transfection efficiencies ranged from 60% to 80%.

The electroporated EWS-96 cells were cultured in 100mm plates and harvested at three timepoints for different sets of experiments – 48 hours, 72 hours and 96 hours post-transfection. The cells were harvested for protein analysis by Western blot.

At 48 hours post-transfection, cells were split and replated as necessary based on the confluency of the plates. Cells were harvested at 72 hours or 96 hours post-transfection in RIPA2++ cell lysis buffer (20 mM Tris pH 7.6, 10% glycerol, 137 mM NaCl, 0.1% SDS, 1% Triton X100, 2 mM EDTA, 0.5% deoxycholic acid sodium salt with phosphatase inhibitors [1 mM sodium orthovanadate, 50 mM sodium fluoride, 25 mM β-glycerophosphate], protease

inhibitors [10 ug/mL leupeptin, 10 uL/mL aprotinin, 1 mM phenylmethylsulfoxide], and 1 mM dithiothreitol).

2.3.1 *In vitro* cell growth assays for siRNA transfected EWS-96 cells

Cell growth was assessed in transfected cells. I plated the cells in 35mm plates at 0.5 x 10^6 viable cells/mL in triplicate at 72 hours post-transfection. The viable cells were counted at 96 hours post-transfection using a hemacytometer with Trypan blue dye exclusion (1x, used at 0.185 mg/mL). The increase in the numbers of viable cells over 24 hours of growth were calculated for each sample based on the initial number of cells plated (0.5 x 10^6 cells).

2.4 Western blotting

2.4.1 Preparation of cell lysates for analysis by Western blotting

Cell lysates for the transfected, control transfected, and non-transfected cells were prepared in RIPA2++ cell lysis buffer. Cells were homogenized in the RIPA2++ cell lysis buffer and then centrifuged at 10,000 g at 4˚C in order to separate the protein extract from the cellular debris. Cell lysates were collected and stored at -80˚C for protein quantification and analysis by sodium dodecyl sulfate polyacrylamide gel electrophoresis (SDS-PAGE).

2.4.2 Preparation of mouse tissues for analysis by Western blotting

Mouse tissues were collected from mice by Dr. Hélène Paradis and Dr. Robert Gendron; mice from which tissues were collected include: *Tie2/rtTA/Enh* mice, *TRE-HA/TBDN* mice, and mice transgenic for TBDN overexpression, both Dox-induced and non-induced (see section 2.5 for further details). Mouse tissues were prepared in RIPA2++ cell lysis buffer. Tissues were homogenized in the RIPA2++ cell lysis buffer. Tissue homogenates were then centrifuged at 10,000 g at 4˚C in order to separate the protein extract in RIPA2++ cell lysis buffer from the

cellular debris and solids. Supernatants were collected and stored at -80˚C for protein quantification and analysis by sodium dodecyl sulfate polyacrylamide gel electrophoresis (SDS-PAGE).

2.4.3 Western blotting of prepared protein extracts

Concentrations of protein extracts were determined colourimetrically using the Bio-Rad protein dye reagent, followed by measurement of absorbance at 595 nm using a spectrophotometer. Bovine serum albumin (BSA) at defined concentrations was used as a control to generate a standard curve for the purposes of protein quantification.

Western blots were performed by loading a specific amount of protein onto a sodium dodecyl sulfate polyacrylamide gel (SDS-PAGE), 6.5% separating gel and 3.5% stacking gel. The SDS-PAGE gel was ran at a 100 V limit overnight (approximately 16 hours). The proteins in the gel were then transferred to a 0.2 μm nitrocellulose membrane (Bio-Rad Laboratories, Hercules, CA). Protein detection was performed using specific primary antibodies and horseradish peroxidase conjugated secondary antibodies (as described above, see section 2.3). Chemiluminescent detection analysis was performed using Lumiglo (KPL, Gaithersburg, MD), Clarity (Bio-Rad Laboratories, Hercules, CA), or ECL Advance (GE Healthcare, Little Chalfont Buckinghamshire, UK) chemiluminescent substrates. The Kodak Gel Logic 2200 imaging system (Eastman Kodak Company, Rochester, NY) and Carestream MI software were used to conduct densitometry analysis and to determine band intensities. The protein bands were quantified relative to loading controls and expressed as a percentage of control siRNA transfected cells.

2.5 Mouse model overexpressing Tubedown under the inducible endothelial/mesenchymal *Tie2* promoter

The role of TBDN during aging was studied in a bi-transgenic mouse model overexpressing TBDN under the control of the inducible endothelial/mesenchymal *Tie2* promoter (Sato et al. 1995) developed by Dr. Hélène Paradis (Figure 2). Promoter induction was accomplished using doxycycline (Dox; BD Biosciences, Mountain View, CA) administered in the diet (Wall et al. 2004). Dox-induced mice were induced from age 14 months to age 17.5 months (ie. 14 weeks) with Dox at 600 μg/kg. These mice were derived and the expression and activity of the transgene characterized by Dr. Hélène Paradis (unpublished). TBDN overexpressed in bi-transgenic mice under the Dox-inducible *Tie2* promoter carried the human influenza hemagglutinin (HA) tag to distinguish it from endogenous TBDN expression upon analysis by Western blot.

TBDN overexpression was achieved in Dox-induced aged mice transgenic for Tubedown overexpression (*Tie2/rtTA/Enh-TRE/HA-TBDN*) using Dox administered in the diet; this has been confirmed by Dr. Hélène Paradis and Dr. Robert Gendron (Dr. H. Paradis and Dr. R. Gendron, personal communication). Dox-induced and non-induced mice (*Tie2/rtTA/Enh* and *TRE/HA-TBDN* and *Tie2/rtTA/Enh-TRE/HA-TBDN*) were used as control groups. The *Tie2/rtTA/Enh* genotype is abbreviated as *HHrtTAXK* in the Paradis/Gendron lab.

2.6 Paraffin-embedded tissue sectioning

Tissues collected from experimental and control mice were fixed by incubations in 4% paraformaldehyde in PBS, followed by 70% ethanol. Fixed tissues were then embedded in paraffin and sectioned using a microtome at a thickness of 5 μm. Tissue sections were floated on water at 40˚C and affixed in pairs to 3-triethoxysilylpropylamine (TESPA)-coated slides. These slides were dried flat or vertically and heated for 2-6 hours at 45˚C to fix the tissue to the slide. Slides were stored vertically in slide boxes until ready for use.

2.7 Hematoxylin and Eosin (H&E) staining

Hematoxylin and eosin (H&E) staining was performed according to a protocol optimized in the Paradis/Gendron lab. Slides were placed vertically into plastic slide racks. Sections were deparaffinized using xylene, then rehydrated in decreasing concentrations of ethanol. The sections were then post-fixed in 4% paraformaldehyde in PBS and rinsed in water. Hematoxylin stain was administered for 13 minutes followed by a rinse in water adjusted to pH 9 with ammonium hydroxide. Eosin stain was administered for 45 seconds, followed by a rinse in water. The sections were dehydrated in increasing concentrations of ethanol, then held in xylene before cover slip mounting with Permount. Slides were allowed to dry overnight in the chemical fumehood before storing flat in a slide folder for microscope analysis.

2.8 Immunohistochemistry

2.8.1 Immunohistochemical analysis of Tubedown expression

Immunohistochemistry analysis of Tubedown (TBDN) expression was performed on mouse tissue sections. Mouse tissues were embedded in paraffin blocks and manually sectioned using a microtome at a thickness of 5 μm and affixed to coated slides. Tissue sections were deparaffinized in xylene and rehydrated in decreasing concentrations of ethanol. Tissue sections

were then incubated with the TBDN monoclonal antibody (OE5 purified immunoglobulin; Martin et al. 2007; developed in Paradis/Gendron lab; used at 12 μg/mL) or an isotype-matched IgG2a negative control monoclonal antibody (UPC-10; mouse IgG2a, kappa, purified immunoglobulin; Sigma, St. Louis, MO; used at 12 μg/mL) overnight, followed by an incubation with anti-mouse IgG2a specific alkaline phosphatase (AP)-conjugated secondary antibody (Vector Laboratories, Inc., Burlingame, CA). Tissue sections were developed for staining using AP substrate Vector Red (Vector Laboratories, Inc., Burlingame, CA). A minimum of three tissue sections were used in each experiment: mouse tumor tissue stained with OE5; control normal mouse tissue stained with OE5; and control normal mouse tissue stained with UPC-10.

2.8.2 Immunohistochemical analysis of proliferating cell nuclear antigen (PCNA) expression

Immunohistochemistry analysis of proliferating cell nuclear antigen (PCNA) expression was performed on mouse tissue. Mouse tissues were embedded in paraffin blocks and manually sectioned using a microtome at a thickness of 5 μm and affixed to coated slides. Tissue sections were deparaffinized in xylene and rehydrated in decreasing concentrations of ethanol. Tissue sections were then incubated with anti-PCNA rabbit polyclonal antibody obtained from Santa Cruz Biotechnology (FL-261; sc-7907; Santa Cruz, CA; 2 μg/mL) or vehicle control, followed by an incubation with anti-rabbit IgG specific alkaline phosphatase (AP)-conjugated secondary antibody (Promega, Madison, WI; 5 μg/mL). Tissue sections were developed for staining using AP substrate Vector Red (Vector Laboratories, Inc., Burlingame, CA). Negative and positive control tissues were run in each experiment to assure specificity.

2.9 Statistical analyses

Statistical analysis was performed using the one-way analysis of variance (*ANOVA*) followed by the Tukey's multiple comparisons test or uncorrected Fisher's exact statistical test. P values were calculated using the PRISM6 program and a P value of less than 0.05 was considered statistically significant. *ANOVA* results were indicated as follows: *, $P < 0.05$; **, $P < 0.005$; ***, $P < 0.0005$; ****, $P < 0.0001$.

Chapter 3 Results

3.1 The role of Tubedown and Arrest-defective-1 in the regulation of p53 levels and cell proliferation in Ewing's sarcoma EWS-96 cells *in vitro*

3.1.1 Tubedown is significantly knocked down in Ewing's sarcoma EWS-96 cells using an siRNA knockdown approach.

Tubedown (TBDN) was discovered as a developmentally regulated protein, and has been shown to be highly expressed in primitive bone tumors of mesenchymal and neuroectodermal origin including osteosarcoma (OS) and Ewing's sarcoma (EWS) (Kalvik and Arnesen 2013, Martin et al. 2007, Starheim and Gromyko et al. 2009; Dr. H. Paradis, personal communication). In order to investigate the role of Tubedown (TBDN) in the p53 tumor suppressor pathway in cancer, we used an *in vitro* siRNA knockdown approach in an Ewing's sarcoma cell line.

At 72 hours post-transfection, TBDN was knocked down by 84% in Ewing's sarcoma EWS-96 cells transfected with *TBDN* siRNA when compared to control cells (Figure 3B; blue, *ANOVA*, $P < 0.0005$). At 96 hours post-transfection, TBDN was knocked down by 65% in Ewing's sarcoma EWS-96 cells transfected with *TBDN* siRNA when compared to control cells (Figure 3C; blue, *ANOVA*, $P < 0.0005$). TBDN was significantly knocked down in Ewing's sarcoma EWS-96 cells by transient siRNA transfection with 10nM of *TBDN* siRNA, when compared to Ewing's sarcoma EWS-96 cells transfected with no siRNA or control siRNA and non-transfected cells (Figure 3). As I used a transient siRNA knockdown approach, the suppression of TBDN expression in our Ewing's sarcoma EWS-96 cells was sustained for a finite time post-transfection. *TBDN* siRNA obtained a statistically significant knockdown of TBDN expression at 72 and 96 hours post-transfection compared to controls.

3.1.2 Tubedown knockdown in Ewing's sarcoma EWS-96 cells suppresses ARD1 levels and induces p53 levels.

In Ewing's sarcoma EWS-96 cells transfected with *TBDN* siRNA we achieved a statistically significant knockdown of TBDN expression (Figure 3B; blue, *ANOVA*, $P < 0.0001$). In comparison to cells transfected with control siRNA, no siRNA, or non-transfected controls, Ewing's sarcoma EWS-96 cells transfected with *TBDN* siRNA showed downregulation in the expression of NatA catalytic subunit ARD1 at both 72 hours and 96 hours post-transfection (Figure 3B; green, *ANOVA*, $P < 0.05$) (Figure 3C; green, *ANOVA,* $P < 0.0005$). TBDN is the regulatory subunit of the NatA complex and it is known that TBDN regulates the activity of ARD1. Suppression of both TBDN and ARD1 expression was observed when cells were transfected with a *TBDN* siRNA. The knockdown of both TBDN and ARD1 upon transfection with the *TBDN*-specific siRNA duplex confirms the interconnected expression of regulatory subunit TBDN and catalytic subunit ARD1 in the acetyltransferase complex NatA.

Further, we observed an upregulation in the expression of the tumor suppressor p53 in Ewing's sarcoma EWS-96 cells transfected with *TBDN* siRNA at both 72 hours and 96 hours post-transfection, when compared to cells transfected with control siRNA, no siRNA, or non-transfected cells (Figure 3B; red, *ANOVA*, $P < 0.05$) (Figure 3C; red, *ANOVA*, $P < 0.005$). Ewing's sarcoma EWS-96 cells with suppressed TBDN expression show an induction in the expression of p53. This suggests that Ewing's sarcoma cells require TBDN expression, either individually or as a component of the NatA complex, in order to suppress p53 expression and overcome tumor suppression.

(A)

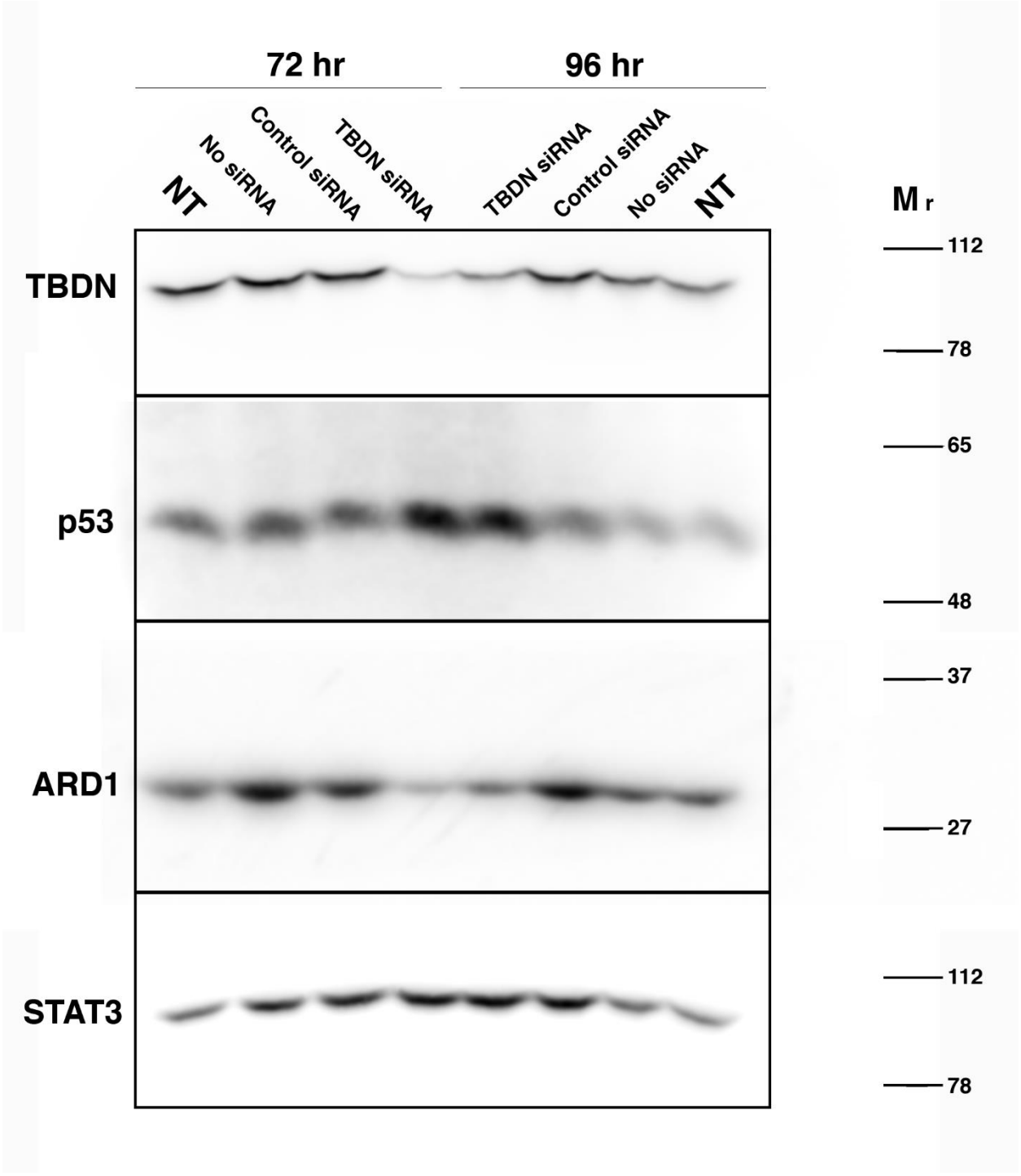
72 hr
96 hr
NT
No siRNA
Control siRNA
TBDN siRNA
TBDN siRNA
Control siRNA
No siRNA
NT
M r
TBDN
p53
ARD1
STAT3
112
78
65
48
37
27
112
78

(B)

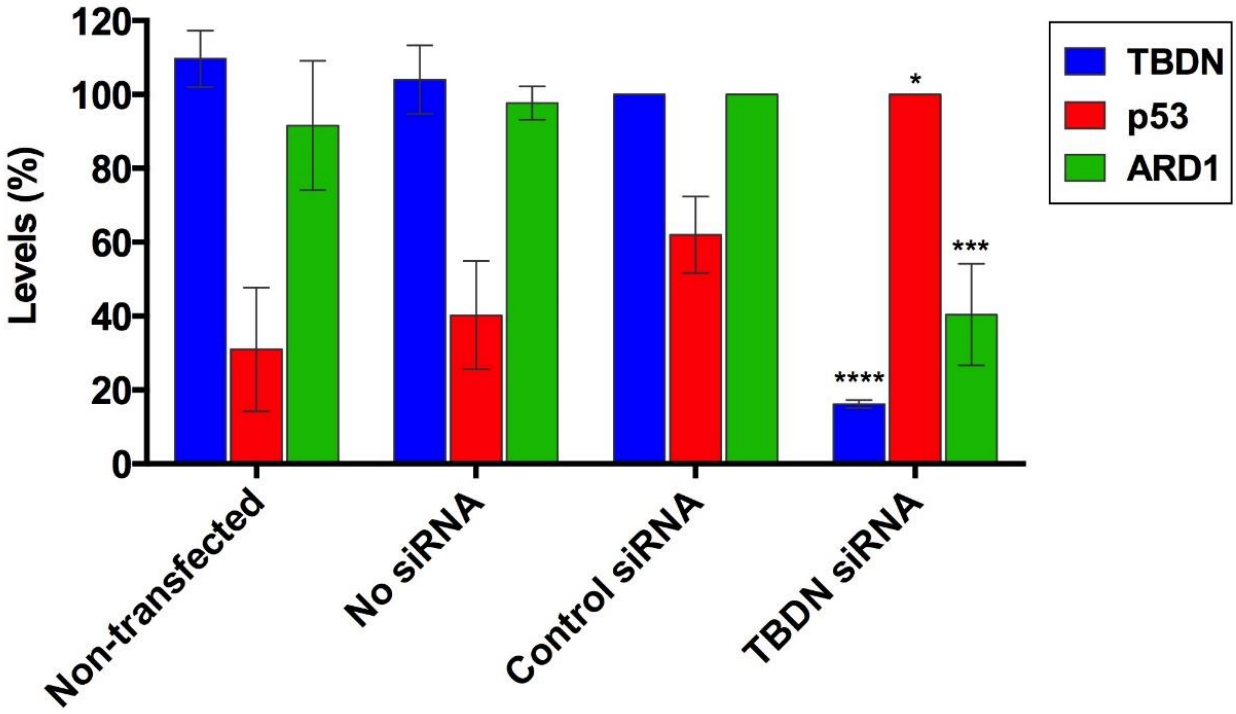
Levels (%)
120
100
80
60
40
20
0
TBDN
p53
ARD1
*
***
****
Non-transfected
No siRNA
Control siRNA
TBDN siRNA

(C)

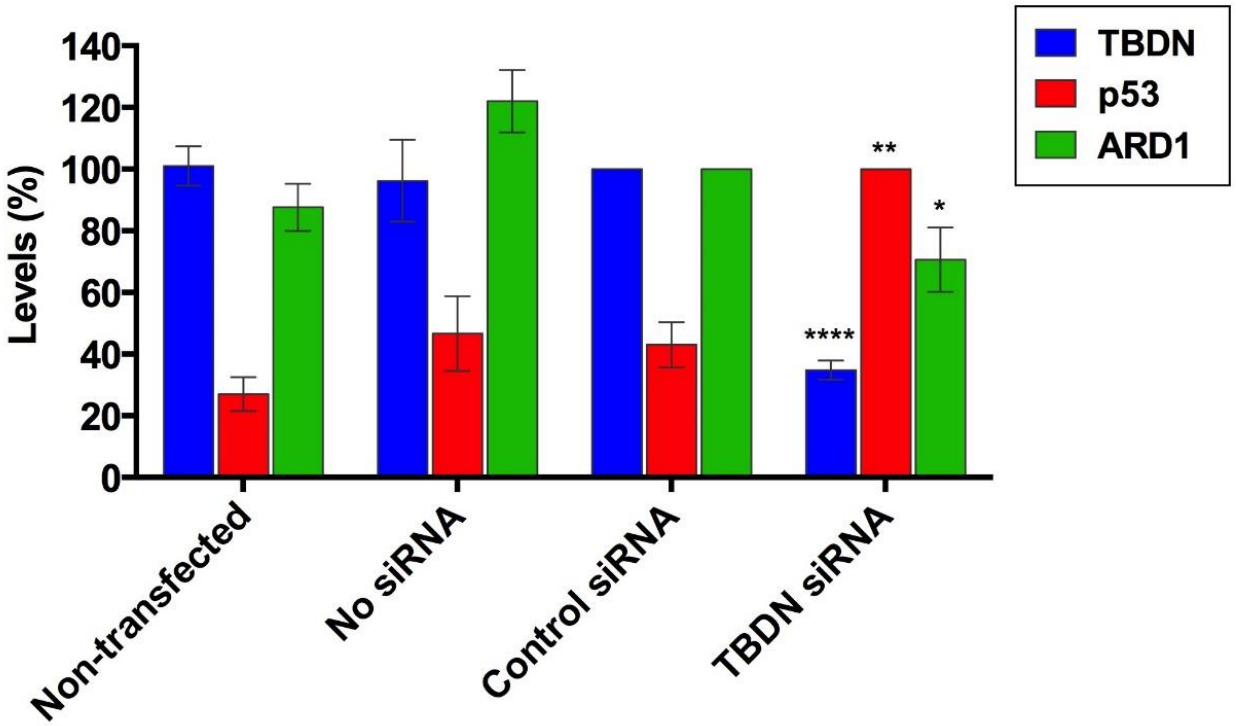
Levels (%)
140
120
100
80
60
40
20
0
TBDN
p53
ARD1
**
*
****
Non-transfected
No siRNA
Control siRNA
TBDN siRNA

Figure 3. Tubedown knockdown in Ewing's sarcoma EWS-96 cells suppresses Arrest-defective-1 protein levels and induces p53 levels.

Ewing's sarcoma EWS-96 cells were transiently transfected with either no siRNA, control siRNA, or *TBDN* siRNA and harvested at 72 hours post-transfection or 96 hours post-transfection. Western blots were performed to determine levels of Tubedown (TBDN), p53, Arrest-defective-1 protein (ARD1), and loading control STAT3 in the cell lysates. **(A)** Representative Western blot. NT, non-transfected. M_r, relative molecular weight. **(B)** Quantitation of Western blots performed using cell lysates harvested at 72 hours post-transfection. Average levels $\pm$ SEM of 4 experiments. **(C)** Quantitation of Western blots performed using cell lysates harvested at 96 hours post-transfection. Average levels $\pm$ SEM of 4 experiments. *ANOVA*; *, $P < 0.05$; **, $P < 0.005$; ***, $P < 0.0005$; ****, $P < 0.0001$.

TBDN levels in the *TBDN* siRNA transfected cells were downregulated at 72 hours and 96 hours post-transfection in comparison to levels in the controls (blue; *ANOVA,* $P < 0.0001$). ARD1 levels in the *TBDN* siRNA transfected cells were downregulated at 72 hours and 96 hours post-transfection in comparison to levels in the controls *(*green; 72 hours: *ANOVA,* $P < 0.005$; 96 hours: *ANOVA,* $P < 0.05$*)*. p53 levels in the *TBDN* siRNA transfected cells were significantly upregulated at 72 hours and 96 hours post-transfection in comparison to levels in the controls (red; 72 hours: *ANOVA,* $P < 0.05$; 96 hours: *ANOVA,* $P < 0.005$). There was no significant difference in TBDN, ARD1, or p53 expression between non-transfected cells and the cells transfected with no siRNA or control siRNA; this is consistent at 72 hours and 96 hours post-transfection.

3.1.3 Arrest-defective-1 protein is significantly knocked down in Ewing's sarcoma EWS-96 cells using an siRNA knockdown approach.

Arrest-defective-1 protein (ARD1) is the catalytic subunit of NatA; the activity of this subunit is regulated by the activity of TBDN (Liszczak et al. 2013; Magin et al. 2016). The mechanistic role of ARD1 in cancer has not been clarified. In order to investigate the role of ARD1 in the p53 tumor suppressor pathway in cancer, we used an *in vitro* siRNA knockdown approach in the EWS-96 Ewing's sarcoma cell line. ARD1 expression was knocked down by 30% in Ewing's sarcoma EWS-96 cells transfected with *ARD1* siRNA, when compared to cells transfected with control siRNA (Figure 4B; green, *ANOVA*, $P < 0.0005$). ARD1 was significantly knocked down by transient siRNA transfection of *ARD1* siRNA at 96 hours post-transfection, when compared to Ewing's sarcoma EWS-96 cells transfected with control siRNA (Figure 4).

There was no effect on TBDN expression in cells transfected with *ARD1* siRNA in comparison to cells transfected with control siRNA or no siRNA (Figure 4B; blue, *ANOVA*, P = n.s.). This result is consistent with previous analyses conducted in the Paradis/Gendron lab, where knocking down ARD1 expression in Ewing's sarcoma EWS-96 cells by *ARD1* siRNA had no impact on the expression of NatA regulatory subunit TBDN.

3.1.4 Arrest-defective-1 protein knockdown in Ewing's sarcoma EWS-96 cells induces p53 levels.

I performed Western blot analysis on cell lysates collected from Ewing's sarcoma EWS-96 cells transfected with *ARD1* siRNA, control siRNA, and no siRNA, in addition to non-transfected EWS-96 cells. In Ewing's sarcoma EWS-96 cells transfected with *ARD1* siRNA we achieved a statistically significant knockdown in ARD1 expression in comparison to cells transfected with control siRNA (Figure 4B; green, *ANOVA*, $P < 0.05$). Ewing's sarcoma EWS-

96 cells transfected with *ARD1* siRNA also showed an upregulation in the expression of p53 at 96 hours post-transfection, in comparison to cells transfected with control siRNA (Figure 4B; red, *ANOVA*, $P < 0.005$). Ewing's sarcoma EWS-96 cells with suppressed ARD1 expression showed induction of the expression of p53. This suggests that Ewing's sarcoma cells require ARD1 expression, either individually or as a component of the NatA complex, in order to suppress p53 expression and circumvent tumor suppression.

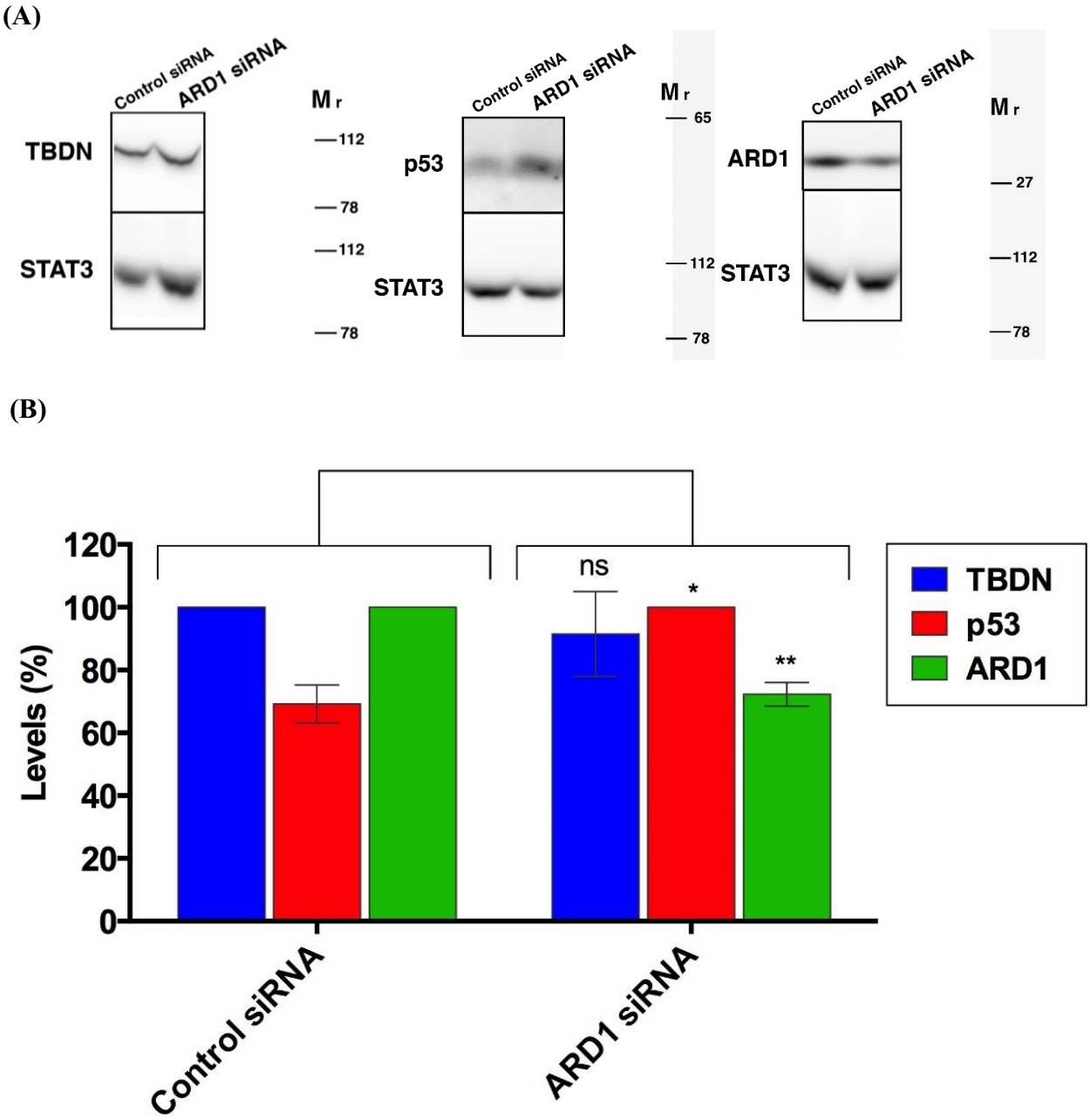

Figure 4. Arrest-defective-1 protein knockdown in Ewing's sarcoma EWS-96 cells induces p53 levels.

Ewing's sarcoma EWS-96 cells were transiently transfected with either control siRNA or *ARD1* siRNA and harvested at 96 hours post-transfection. Western blots were performed to determine levels of Arrest-defective-1 protein (ARD1), p53, Tubedown (TBDN), and loading control

STAT3 in the cell lysates. Dr. Hélène Paradis (Faculty of Medicine, Memorial University) assisted with cell transfections and data analysis. **(A)** Representative Western blot. NT, non-transfected. M_r, relative molecular weight. **(B)** Quantitation of Western blots performed using cell lysates harvested at 96 hours post-transfection. Average levels $\pm$ SEM of 4 experiments. *ANOVA*; *, $P < 0.05$; **, $P < 0.005$; ***, $P < 0.0005$; ****, $P < 0.0001$.

ARD1 levels in the *ARD1* siRNA transfected cells were downregulated in comparison to levels in the control (green; *ANOVA*, $P < 0.005$). There was no significant difference in TBDN levels in the *ARD1* siRNA transfected cells in comparison to levels in the controls *(*blue; *ANOVA*, P = n.s.). p53 levels in the *ARD1* siRNA transfected cells were significantly upregulated in comparison to levels in the cells transfected with control siRNA (red; *ANOVA*, $P < 0.05$).

3.1.5 Knockdown of Tubedown or Arrest-defective-1 protein suppresses proliferation of Ewing's sarcoma EWS-96 cells *in vitro*.

I performed an *in vitro* cell growth assay with the Ewing's sarcoma EWS-96 cell line in order to compare the cell proliferation and growth capacity of cells with knocked down TBDN and ARD1 expression in comparison to control transfected cells. Based on the initial known inoculum of 500,000 viable cells, we quantified cell growth between 72 hours and 96 hours post-transfection and compared the increase in the number of viable cells seen in cells transfected with *TBDN*-specific or *ARD1*-specific siRNA to that of control transfected cells. We quantified 'cell growth' as a percentage relative to the increase in the number of viable cells seen in our control siRNA transfected cells.

In Ewing's sarcoma EWS-96 cells transfected with *TBDN* siRNA we achieved a statistically significant knockdown in TBDN expression (Figure 5; red, *ANOVA*, $P < 0.0005$). In comparison to control transfected cells, we observed a statistically significant decrease in cell growth in cells with suppressed TBDN expression (Figure 5; blue, *ANOVA*, $P < 0.05$).

In Ewing's sarcoma EWS-96 cells transfected with *ARD1* siRNA we achieved a statistically significant knockdown in ARD1 expression (Figure 6; red, *ANOVA*, $P < 0.05$). We observed a statistically significant decrease in cell growth in cells with knocked down ARD1 expression, when compared to control transfected cells (Figure 6; blue, *ANOVA*, $P < 0.05$).

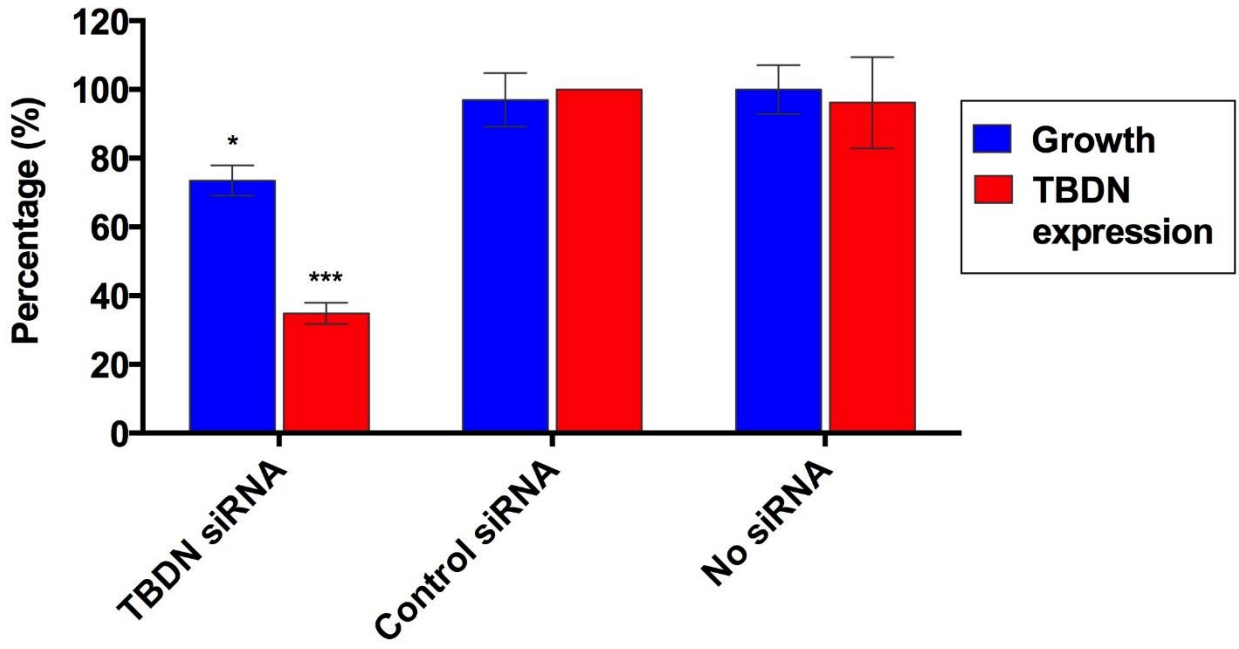

Figure 5. Tubedown knockdown in Ewing's sarcoma EWS-96 cells reduces cell growth.

Ewing's sarcoma EWS-96 cells were transiently transfected with either no siRNA, *TBDN* siRNA, or control siRNA. Initial inoculates of 0.5 million cells were plated in triplicate for each treatment at 72 hours post-transfection. Cells were counted using a hemacytometer at 96 hours post-transfection, after 24 hours of growth. The total number of viable cells in each plate were counted and expressed as a percentage relative to the number of new viable cells seen in the no siRNA transfected cells. Average cell growth percentage levels $\pm$ SEM; n = 4. *ANOVA*; *, $P < 0.05$; **, $P < 0.005$; ***, $P < 0.0005$.

Cell growth was reduced in *TBDN* siRNA transfected cells in comparison to control transfected cells (ANOVA, $P < 0.05$; n = 4). There was no significant difference in cell growth between the cells transfected with no siRNA or control siRNA.

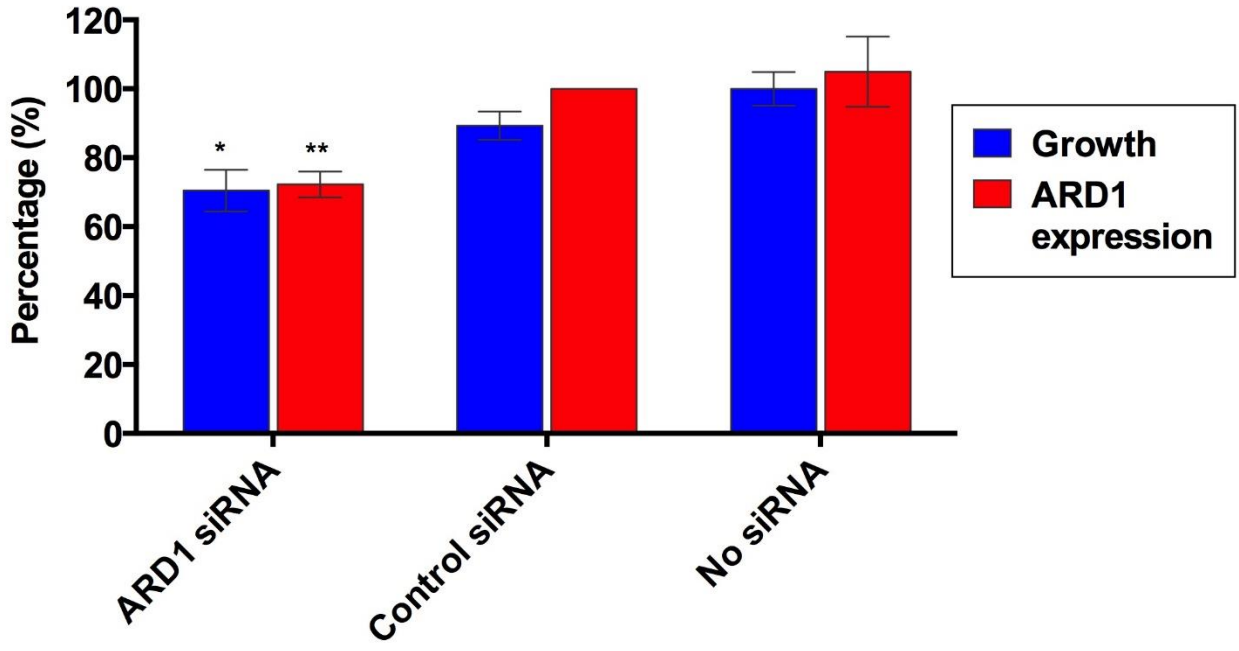

Figure 6. Arrest-defective-1 protein knockdown in Ewing's sarcoma EWS-96 cells reduces cell growth.

Ewing's sarcoma cells were transiently transfected with either no siRNA, *ARD1* siRNA, or control siRNA. Initial inoculates of 0.5 million cells were plated in triplicate for each treatment at 72 hours post-transfection. Cells were counted using a hemacytometer at 96 hours post-transfection, after 24 hours of growth. The total number of viable cells in each plate were counted and expressed as a percentage relative to the number of new viable cells seen in the no siRNA transfected cells. Average cell growth percentage levels $\pm$ SEM; n = 6. *ANOVA*; *, $P < 0.05$; **, $P < 0.005$; ***.

Cell growth was reduced in *ARD1* siRNA transfected cells in comparison to the control transfected cells (ANOVA, $P < 0.05$; n = 6). There was no significant difference in growth seen between cells transfected with no siRNA and control siRNA.

Ewing's sarcoma EWS-96 cells with knocked down TBDN or ARD1 expression showed a statistically significant reduction in cell proliferation when compared to cells transfected with control siRNA or no siRNA, and non-transfected cells (Figures 5 and 6; *ANOVA*, $P < 0.05$). These data indicate that Ewing's sarcoma cells require expression of TBDN and ARD1, either individually or in complex as the acetyltransferase NatA, in order to promote cancer cell growth *in vitro*.

3.1.6 Tubedown is involved in the regulation of p53 expression and cell proliferation in Ewing's sarcoma EWS-96 cells.

We have determined that Ewing's sarcoma EWS-96 cells knocked down for TBDN or ARD1 expression showed upregulated p53 expression and a reduction in cell proliferation when compared to cells transfected with control siRNA or no siRNA or non-transfected cells. These data suggest that ARD1 and TBDN are required for the downregulation of p53 and the promotion of cancer cell growth in Ewing's sarcoma cells.

3.2 Tubedown in the regulation of p53 expression in mice during aging

TBDN is a novel homeostatic factor involved in blood vessel growth and homeostasis (Gendron et al. 2000, Gendron et al. 2001, Paradis et al. 2002, Wall et al. 2004). During aging, there is a notable decrease in the levels of TBDN expression, specifically in the retinal and choroidal vasculature; this contributes to the development of age-related retinopathy (Gendron et al. 2010). During aging there is an increase in oxidative damage and DNA damage present in cells; this activates p53 and results in the presence of increased p53 protein levels in the tissues of aging mice (Rufini et al. 2013). Based on the data collected *in vitro* using the Ewing's sarcoma EWS-96 cell line, there is a link between knocked down TBDN expression and increased expression of the the tumor suppressor p53 (Figures 3-4; Dr. H. Paradis, personal communication). This suggests that cancer cells require TBDN in order to downregulate p53, bypass p53 tumor suppression, and promote cancer cell growth. As a continuation of this investigation, we wanted to investigate the effects of TBDN overexpression on the regulation of the p53 pathway during aging *in vivo*.

In order to investigate the role of TBDN during aging in mice, we used a bi-transgenic mouse model overexpressing TBDN under the control of the inducible endothelial/mesenchymal *Tie2* promoter (section 2.5, Figure 2; Dr. H. Paradis, unpublished; Wall et al. 2004). Doxycycline (Dox) administered in the diet was used for promoter induction. The three genotypes of mice derived by Dr. Hélène Paradis include: *HHrtTAXK-TRE/HA-TBDN*, mice transgenic for Tubedown overexpression when induced with Dox; and *HHrtTAXK* and *TRE/HA-TBDN*, the control mice. Dox-induced and non-induced mice were collected for each genotype. The groups of mice we used in this study include aged mice transgenic for Tubedown expression and control mice (wildtype, *HHrtTAXK*, and *TRE/HA-TBDN*), both Dox-induced and non-

induced. It has been confirmed previously that expression of the HA-TBDN cDNA construct is seen in TBDN-overexpressing transgenic mice, and not in our single transgenic control groups (Dr. H. Paradis, personal communication). This transgenic mouse model was developed and the activity of the transgene confirmed by Dr. Hélène Paradis, and tissues were provided for analysis in this study.

Using this bi-transgenic mouse model established in the Paradis/Gendron lab, I wanted to investigate the effects of TBDN overexpression during aging in the context of the p53 tumor suppression pathway.

3.2.1 Dox-induced aged mice transgenic for Tubedown overexpression show abnormal growths in unique tissues in comparison to control aged mice.

Abnormal tissue growths that had been collected by Dr. Hélène Paradis and Dr. Robert Gendron (Faculty of Medicine, Memorial University) from aged mice – *HHrtTAXK* control aged mice, *TRE/HA-TBDN* control aged mice, non-induced aged mice transgenic for TBDN overexpression (*HHrtTAXK-TRE/HA-TBDN*), and Dox-induced aged mice transgenic for TBDN overexpression (*HHrtTAXK-TRE/HA-TBDN*) – were analyzed and categorized by Dr. Hélène Paradis (Table 1).

In Dox-induced aged mice transgenic for TBDN overexpression (genotype *HHrtTAXK-TRE/HA-TBDN*) abnormal growths collected in the total cohort thus far equate to 23.8% incidence (15 abnormal growths collected, n = 63; Table 1). The control aged mice (*HHrtTAXK* and *TRE/HA-TBDN* control aged mice) showed lower incidence of abnormal growths than the Dox-induced aged mice transgenic for TBDN overexpression (Table 1). Notably, abnormal growths were only found in the lung tissue of the *HHrtTAXK* control aged mice and non-induced *HHrtTAXK-TRE/HA-TBDN* aged mice transgenic for TBDN overexpression (Table 1, italicized

text). No abnormal growths have been found so far in the *TRE-HA/TBDN* control aged mice (Table 1). In the Dox-induced aged mice transgenic for TBDN overexpression, abnormal growths were collected from 8 different tissues, including lung (Table 1, red highlighted text).

Abnormal lung growths were found to occur during aging in the *HHrtTAXK* control aged mice as well as in the Dox-induced and non-induced aged mice transgenic for TBDN overexpression (genotype *HHrtTAXK-TRE/HA-TBDN*) (Dr. H. Paradis, personal communication). Based on this determination, we postulated that lung tumors may occurred spontaneously with aging in our cohort of mice and may not be directly induced by a pathway related to the overexpression of TBDN under the inducible endothelial/mesenchymal *Tie2* promoter. I wanted to analyze abnormal growths which were induced by a mechanism related to the overexpression of TBDN in the Paradis/Gendron transgenic mouse model under the control of the endothelial/mesenchymal *Tie2* promoter in our Dox-induced aged mice transgenic for TBDN overexpression. This provided the basis for excluding lung tumors from our analysis and focussing on abnormal growths arising in tissues unique to Dox-induced aged mice transgenic for TBDN overexpression. For further histological and immunohistochemical analysis, I selected two liver growths (mice J.12.7B and L.12.10CM) and one peritoneal growth (mouse H.12.4L) collected from three separate Dox-induced aged mice lines transgenic for TBDN overexpression.

Table 1. Summary of abnormal growths found in different tissues of aged mice.

Abnormal growths found in tissues of aged mice				
Genotype	***HHrtTAXK* control aged mice**	***TRE-HA/TBDN* control aged mice**	**Non-induced aged mice transgenic for Tubedown overexpression**	**Dox-induced aged mice transgenic for Tubedown overexpression**
Tissue from which abnormal growth was collected	*lung*	No abnormal growths collected	*lung*	**liver** **peritoneum** pancreas uterine brain kidney epidydimis *lung*

Data obtained from Dr. Hélène Paradis and Dr. Robert Gendron (Faculty of Medicine, Memorial University). All abnormal growths found in sacrificed mice were collected and prepared for analysis by Dr. Hélène Paradis and Dr. Robert Gendron (Faculty of Medicine, Memorial University). Abnormal growths were found only in aged mice (>16 months old); abnormal growths were not found in the Paradis/Gendron cohort of mice during middle age. Highlighted in red are tissues where abnormal growths were found only in Dox-induced aged mice transgenic for Tubedown overexpression (15 abnormal growths collected, n = 63; 23.8% incidence). Italicized are tissues where abnormal growths were found in control aged mice.

3.2.2 Tubedown expression in the cells and blood vessels of two abnormal liver growths and an abnormal peritoneal 'gut' growth collected from Dox-induced aged mice transgenic for Tubedown overexpression.

I wanted to analyze the histological characteristics and evaluate the expression of TBDN in abnormal growths collected from Dox-induced aged mice transgenic for Tubedown overexpression, in comparison to middle aged and aged tissues collected from *HHrtTAXK* control aged mice. H&E staining provided an image of the histology of the abnormal growth tissues in comparison to control middle aged and aged tissues.

I first analyzed the histological characteristics of two liver growths collected from Dox-induced aged mice transgenic for TBDN overexpression (Figure 7, representative images). The middle aged and aged liver tissues showed uniform distribution of well-defined hepatocytes, and relatively large and regularly distributed blood vessels (Figure 7A-B, representative images). In the aged liver tissue, there was an increase in the area of the tissue occupied by fatty deposits (Figure 7B; appear in images as empty circles/droplets). We postulated that this is "fatty liver" characteristic of aging liver tissues; this also carried over to the liver growth tissue section (Figure 7C, representative image). The liver growths showed abnormal-looking nuclei and areas lacking the characteristics of normal hepatocytes, in their lack of uniformity and uneven distribution (Figure 7C, representative image). The liver growths also showed irregular vasculature, with many irregularly distributed and distended blood vessels (Figure 7C, representative image). The liver growths (Figure 7C, representative image) showed abnormal histology, abnormal vasculature, and less eosinophilic (red) staining than the middle aged liver and aged liver tissues (Figure 7A-B, representative images). Also, there appeared to be a higher number of presumably fatty droplets in the liver growths than in aged liver (Figure 7B-C, representative images).

I also evaluated the expression of TBDN in the cells and blood vessels of abnormal growths in comparison to control tissues. Specifically, we compared the intensity of staining found in the blood vessels and surrounding tissue cells of the growths in comparison to control normal tissue. TBDN immunohistochemistry of growth sections and corresponding control normal tissue sections was performed using a monoclonal antibody against TBDN (referred to as OE5). TBDN staining is indicated by a pink colour.

We performed TBDN staining on the liver growths collected from two Dox-induced aged mice transgenic for TBDN overexpression; our control tissues were middle aged and aged liver from non-induced *HHrtTAXK* control mice. Figure 7 shows representative H&E staining and representative TBDN staining seen in the middle aged liver, aged liver, and abnormal liver growths collected from Dox-induced aged mice transgenic for TBDN overexpression. Faint TBDN staining was isolated to the blood vessels of the control middle aged and aged liver tissues (Figure 7D-E, arrows). In the liver growths collected from two Dox-induced aged mice transgenic for TBDN overexpression, I found intense TBDN staining in both the cells (Figure 7F, arrowheads) and blood vessels (Figure 7F, arrows). This is indicative of the overexpression of TBDN in the cells and blood vessels of both liver growths collected from the Dox-induced aged mice transgenic for TBDN overexpression.

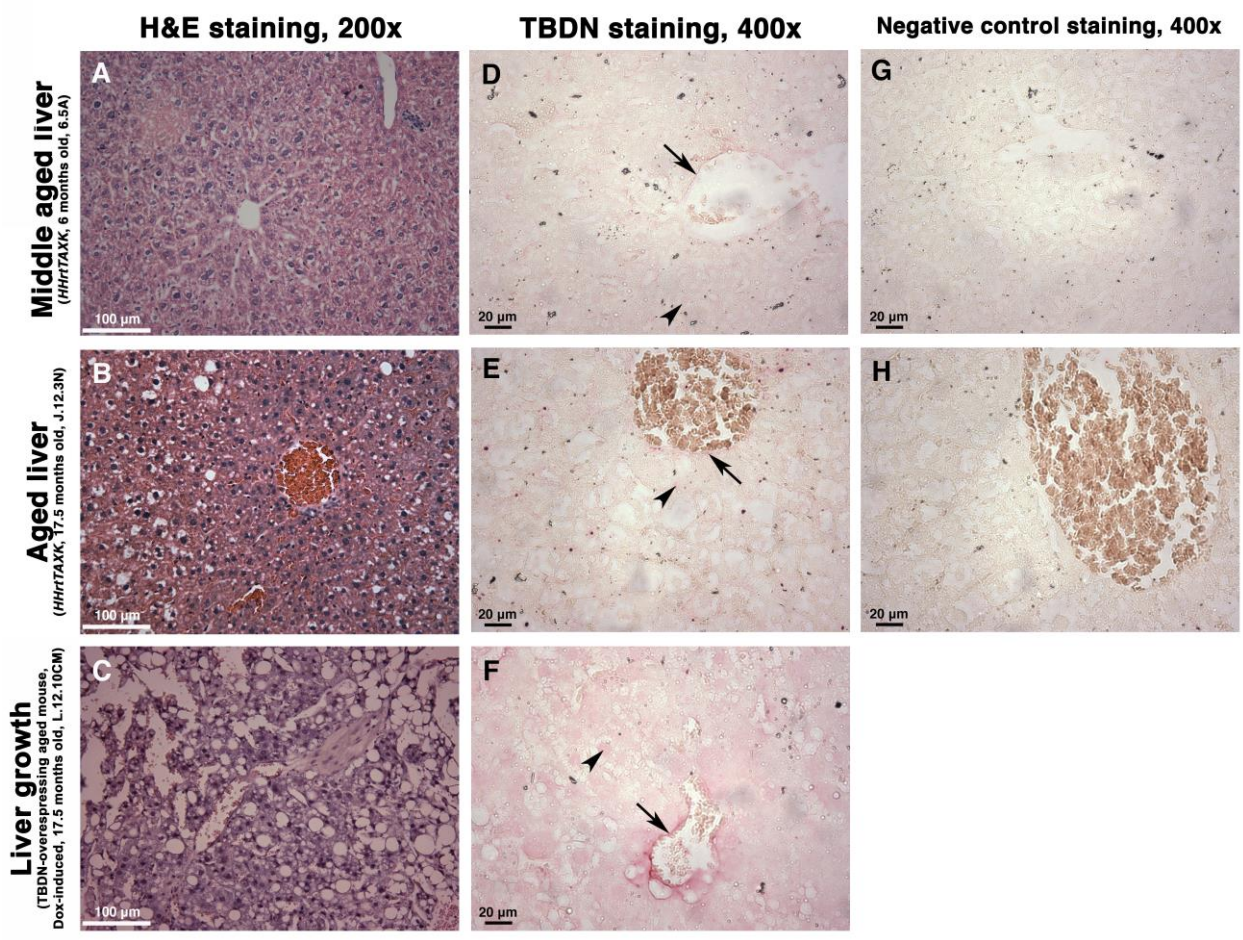

Figure 7. Tubedown overexpression in an abnormal liver growth collected from a Dox-induced aged mouse transgenic for Tubedown overexpression.

Tubedown (TBDN) expression was evaluated by TBDN immunohistochemistry in abnormal liver growths collected from two Dox-induced aged mice transgenic for TBDN overexpression. The above images are representative of the staining observed for both liver growths and their respective control liver tissues (*HHrtTAXK*, non-induced).

Hematoxylin and eosin (H&E) staining (A, B, C) was performed to evaluate histological characteristics of the abnormal liver growth (C) versus middle aged liver (A) and aged liver (B) tissues.

TBDN staining was performed using a TBDN monoclonal antibody, OE5 (D, E, F). Negative control antibody staining was performed using an isotype-matched monoclonal antibody UPC-10 (G and H). Positive TBDN staining is indicated by a pink colour. Arrows point to blood vessel staining (endothelium). Arrowheads point to cell staining. In the normal liver, faint TBDN staining was isolated to the blood vessels (arrows; D, middle aged liver; E, aged liver). TBDN was overexpressed in the blood vessels of the liver growth (arrows; F, liver growth), as well as in the cells of the growth (arrowheads; F, liver growth). TBDN staining was quantified in Figure 9.

I also analyzed H&E staining and TBDN staining of a peritoneal growth collected from a Dox-induced aged mouse transgenic for TBDN overexpression; our control tissues were middle aged spleen, collected from a middle aged wildtype mouse, and middle aged and aged liver tissues collected from non-induced *HHrtTAXK* mice.

I performed H&E staining in order to evaluate the histological characteristics of the peritoneal growth (Figure 8A-D). Based on histological analysis and a literature search, we postulated that this growth found in the gut of a Dox-induced aged mouse transgenic for TBDN overexpression was likely a peritoneal tumor of neuroendocrine origin (Levy et al. 2009). The middle aged spleen, a tissue of neuroendocrine origin, showed characteristic distribution of white pulp (region of dense purple-staining nuclei) and vasculature (Figure 8A). The middle aged and aged liver tissues showed uniform distribution of well-defined hepatocytes, and relatively large and regularly distributed blood vessels (Figure 8B-C). The peritoneal growth showed abnormal histological characteristics, with densely packed large nuclei and unorganized cell distribution, and was highly vascularized by small irregularly shaped blood vessels (Figure 8D). The peritoneal growth also showed more basophilic (purple) staining and less eosinophilic (red) staining when compared to the control liver and spleen tissues (Figure 8A-C). Overall, the peritoneal growth showed abnormal histology, indicated by irregular vascularization, large nuclei, and lack of eosinophilic staining, in comparison to control spleen and liver tissues (Figure 8A-D).

We compared the intensity of staining found in the blood vessels and surrounding tissue cells of the peritoneal growth, in comparison to middle aged spleen, middle aged liver, and aged liver tissues. Faint TBDN staining was isolated to the blood vessels of the middle aged spleen (Figure 8E, arrows). TBDN staining in the middle aged and aged control liver tissue was

isolated to the blood vessels (Figure 8F-G, arrows). In the peritoneal 'gut' growth collected from a Dox-induced aged mouse transgenic for TBDN overexpression, we found intense TBDN staining in the cells (Figure 8H, arrowheads) and blood vessels (Figure 8H, arrows). This is indicative of the overexpression of TBDN throughout the cells and blood vessels of the peritoneal growth collected from the Dox-induced aged mouse transgenic for TBDN overexpression.

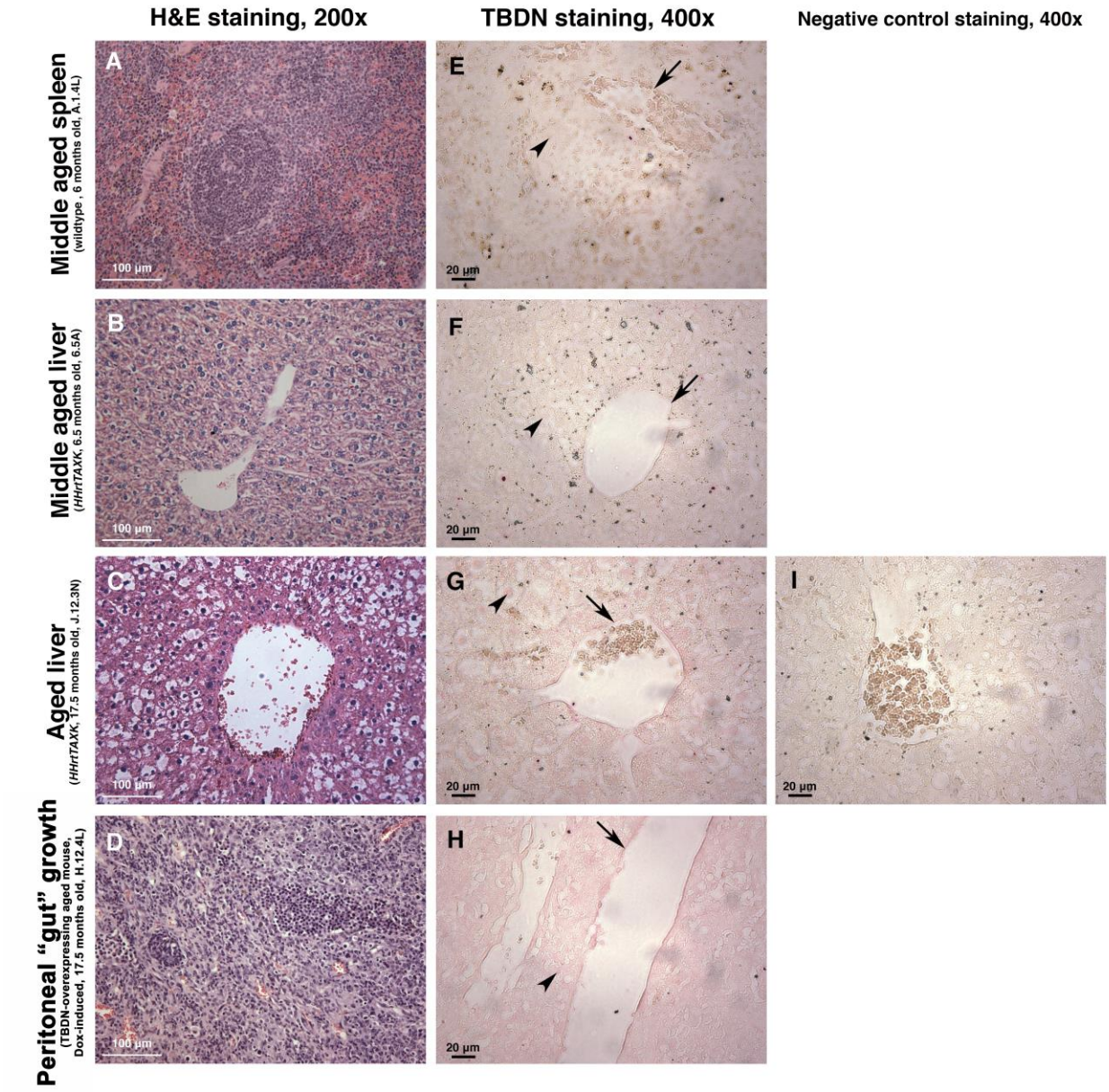

Figure 8. Tubedown overexpression in an abnormal peritoneal growth collected from a Dox-induced aged mouse transgenic for Tubedown overexpression.

Tubedown (TBDN) expression was evaluated by TBDN immunohistochemistry in the abnormal peritoneal growth collected from a Dox-induced aged mouse transgenic for TBDN overexpression. The above images are representative of the staining observed for the peritoneal

growth, and the corresponding control spleen (wildtype, non-induced) and liver tissues (*HHrtTAXK*, non-induced).

Hematoxylin and eosin (H&E) staining (A-D) was performed to evaluate histological characteristics of the peritoneal 'gut' growth (D) versus middle aged spleen (A), middle aged liver (B), and aged liver (C) tissues.

TBDN staining was performed using a TBDN monoclonal antibody, OE5 (E-H). Negative control antibody staining was performed using an isotype-matched monoclonal antibody UPC-10 (I). Positive TBDN staining is indicated by a pink colour. Arrows point to blood vessel staining (endothelium). Arrowheads point to cell staining. In the middle aged spleen, there were low levels of TBDN staining detected in the blood vessels (arrows; E, middle aged spleen). Similarly, in the middle aged and aged liver tissues, faint TBDN staining was isolated to the blood vessels (arrows; F, middle aged liver; G, aged liver). TBDN was overexpressed throughout the peritoneal growth, in both the cells (arrowheads; H, peritoneal growth) and blood vessels (arrows; H, peritoneal growth). Tubedown staining was quantified in Figure 9.

As a whole, we compared TBDN staining seen in middle aged liver and spleen, aged liver, and abnormal growth tissues (livers and peritoneum) collected across all of our TBDN immunohistochemical staining. We saw consistency across our multiple TBDN immunohistochemical stains conducted on separate occasions. There was no statistically significant difference in staining seen between our control middle aged liver tissues collected from multiple mice (data not shown). There was also no statistically significant difference in staining between our control aged liver tissues collected from multiple mice (data not shown). There was no significant difference observed in the TBDN staining of the blood vessels of middle aged tissues when compared to aged tissues (Figure 9A; *ANOVA*, P = n.s.). There was a difference in the TBDN staining observed in the cells of middle aged and aged tissues, with the cells of aged tissues showing more intense TBDN staining (Figure 9B; *ANOVA*, $P < 0.005$).

Based on these data, we compared the combined average TBDN staining seen in the cells and blood vessels of the three abnormal growths tested to the TBDN staining seen in control aged and middle aged tissues. We found that both blood vessel staining and cell staining seen in the abnormal growths collected from the livers and peritoneum of Dox-induced aged mice transgenic for TBDN overexpression was significantly higher than TBDN staining seen in middle aged and aged control tissues (Figure 9; *ANOVA,* $P < 0.0001$). In comparison to middle aged and aged control tissues, Tubedown is overexpressed in the blood vessels and cells of the abnormal growths collected from the livers and peritoneum of three Dox-induced aged mice transgenic for Tubedown overexpression (Figure 9).

(A)

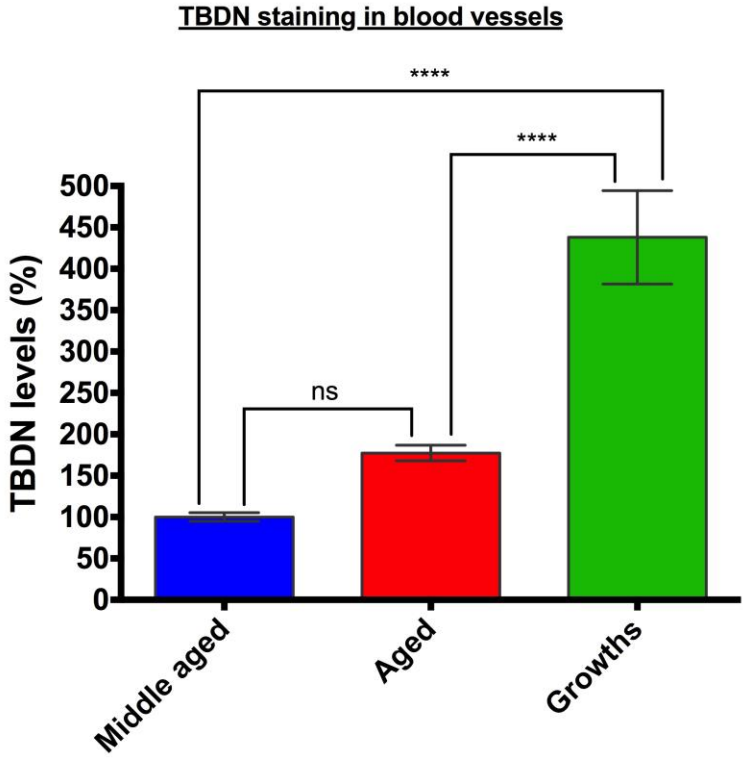
TBDN staining in blood vessels
****
****
ns
TBDN levels (%)
500
450
400
350
300
250
200
150
100
50
0
Middle aged
Aged
Growths

(B)

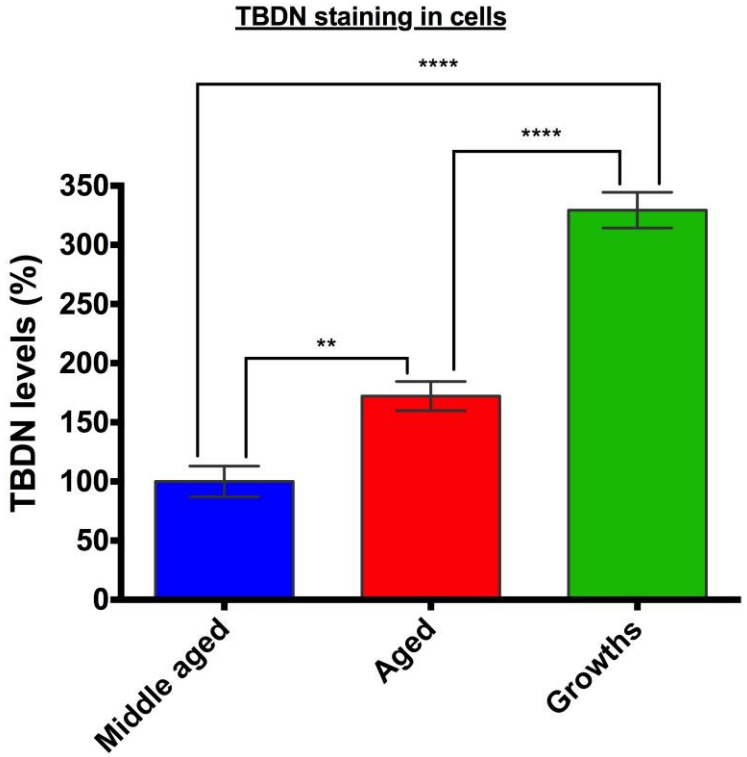
TBDN staining in cells
****
****
**
TBDN levels (%)
350
300
250
200
150
100
50
0
Middle aged
Aged
Growths

Figure 9. Tubedown overexpression in the blood vessels and cells of abnormal growths collected from the livers and peritoneum of Dox-induced aged mice transgenic for Tubedown overexpression.

We performed Tubedown immunohistochemical staining on three abnormal growths collected from the livers and peritoneum of three separate Dox-induced aged mice transgenic for Tubedown overexpression, in comparison to middle aged spleen, middle aged liver, and aged liver tissues. Middle aged spleen, middle aged liver, and aged liver tissues were collected from wildtype and non-induced *HHrtTAXK* control mice. Tubedown staining was performed using a Tubedown monoclonal antibody (OE5). Negative control antibody staining was performed using an isotype-matched monoclonal antibody (UPC-10). We quantified the intensity of Tubedown staining in the blood vessels (A) and cells (B) of each tissue section using red/green ratios in ImageJ software. Average Tubedown levels $\pm$ SEM of at least 6 tissue sections. Middle aged (spleen and liver), n = 10; Aged (liver), n = 6; Growths, n = 6. *ANOVA*; n.s., $P > 0.05$; **, $P < 0.005$; ****, $P < 0.0001$.

Tubedown was overexpressed in the blood vessels (A) and cells (B) of the abnormal growths collected from Dox-induced aged mice transgenic for Tubedown overexpression (green) when compared to middle aged (blue) and aged (red) tissues collected from control mice (*ANOVA*, $P < 0.0001$).

3.2.3 Determining the state of proliferation of cells in abnormal growths collected from Dox-induced aged mice transgenic for Tubedown overexpression in comparison to middle aged and aged liver tissues.

Our histological analysis by H&E staining suggested that the two liver growths and one peritoneal growth collected from three separate Dox-induced aged mice transgenic for TBDN overexpression showed abnormal histological characteristics compared to control tissues, including large irregularly shaped nuclei. Further, my immunohistochemical analysis of TBDN expression in the liver and peritoneal growths showed that TBDN was overexpressed in the cells and blood vessels. The abnormal histology and the overexpression of TBDN in these abnormal growths, when compared to middle aged and aged control tissues, suggested that these are likely tumors.

I wanted to confirm that these abnormal growths were indeed tumors by performing further immunohistochemical analysis looking at the state of proliferation of the cells in these growths collected from Dox-induced aged mice transgenic for TBDN overexpression. I looked at the expression of proliferating cell nuclear antigen (PCNA) in the abnormal growths, in comparison to middle aged and aged control tissues. PCNA is a known marker of cell proliferation; an increase in PCNA expression is indicative of cell growth, but can also indicate DNA damage in the absence of normal cell cycle functions (Bologna-Molina et al. 2013). In normal aged tissues, I did not expect to see high levels of PCNA expression; there is little proliferation occurring with the cells of aging control liver tissue, as the cells enter senescence and reach the end of their replicative life cycle, and it is known that PCNA expression is indicative of cells in the G1/S phase of the cell cycle (Bologna-Molina et al. 2013). In comparing PCNA staining in our control aged tissues to PCNA staining in our abnormal growths collected from Dox-induced aged mice transgenic for TBDN overexpression, I elucidated the

state of proliferation of the cells in these growths and was able to confirm with greater certainty that these abnormal growths are likely tumors.

Figure 10 shows PCNA staining of middle aged liver, aged liver, and abnormal growth tissue representative of all three of our abnormal growths (two liver growths and one peritoneal growth). I observed the expression of PCNA throughout liver tissues collected from middle aged control mice (age 6 months) (Figure 10A). PCNA staining was intense nuclear staining isolated to the nuclei of the cells, and distributed evenly in all parts of the tissue sections with little variation in staining intensity from cell-to-cell. I observed significantly lower levels of PCNA expression in aged liver (17.5 months old) and spleen tissues collected from control mice, but there was no change in the overall distribution of the PCNA staining evenly throughout the tissue sections and again little variation in staining intensity from cell-to-cell (Figure 10B). This is indicative of the presence of a low level of proliferation in the liver tissues of our aged mice, as expected in normal aging tissues. Upon examination of our two abnormal liver growths and one peritoneal growth, I confirmed higher intensity expression of PCNA and changes in the distribution of PCNA staining in these abnormal tissue growths, in comparison to the PCNA expression observed in the liver tissue of middle aged and aged mice (Figure 10C, representative PCNA staining seen across the three abnormal growths). I observed highly specific expression of PCNA staining in certain parts of the section, unlike the evenly distributed staining which I observed in the control liver tissues, and somewhat variable staining intensity from cell-to-cell. Some regions of the growth showed high intensity nuclear PCNA staining in concentrated pockets of cells, while other areas showed a lower level of staining in more dispersed cells. Upon quantifying the PCNA staining intensity, I observed significantly higher PCNA expression in both abnormal liver growths and the abnormal peritoneal growth, when compared to control

aged liver tissue (Figure 11; *ANOVA,* $P < 0.005$). This is indicative of abnormally increased proliferation occurring in the cells of these growths.

Paired with my earlier histological and TBDN immunohistochemistry analysis of these growths, PCNA immunohistochemistry confirmed that the cells in these tissues show additional characteristics of cancer cells. Based on analysis of PCNA expression, the data suggests that the cells in the liver growths and the peritoneal growth are proliferating irregularly when compared to normal aged tissues. This further substantiates my histological identification of these abnormal growths as tumors.

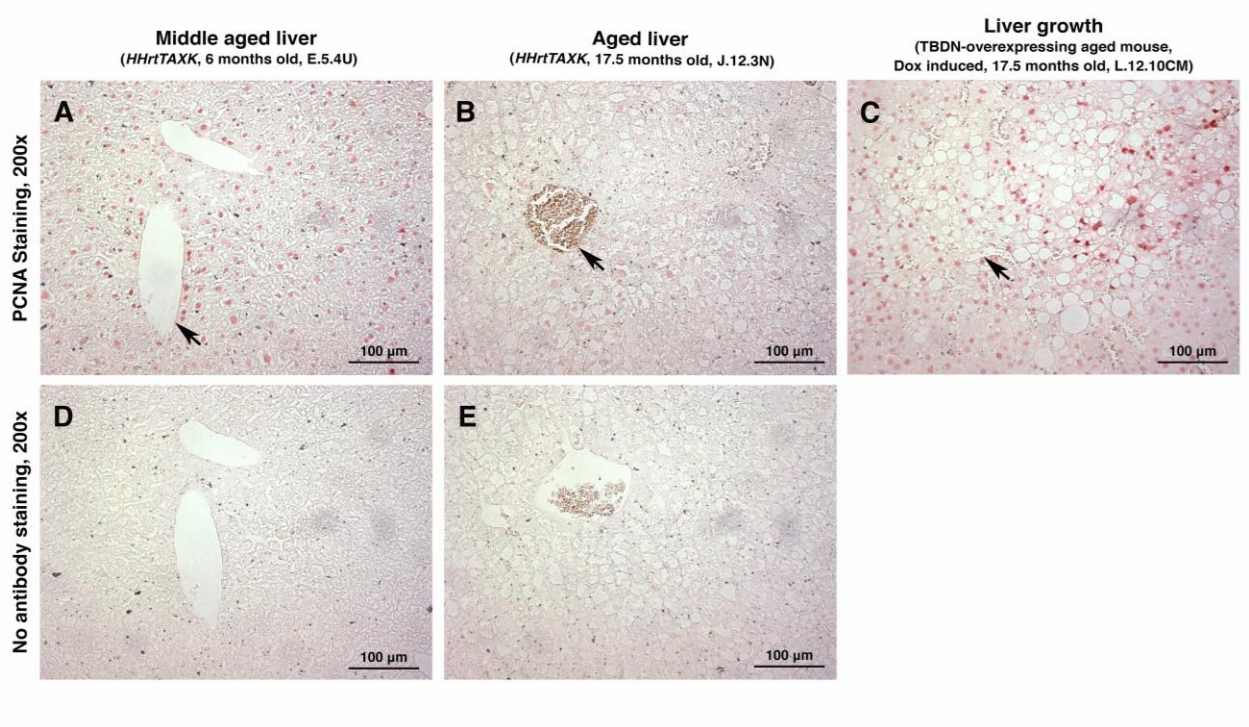

Figure 10. Abnormal cell proliferation in an abnormal liver growth collected from a Dox-induced aged mouse transgenic for Tubedown overexpression suggested by PCNA immunohistochemistry.

Staining for the proliferation marker proliferative cell nuclear antigen (PCNA) was conducted on control middle aged and aged liver tissues in comparison to the abnormal growths collected from the livers and peritoneum of Dox-induced aged mice transgenic for Tubedown overexpression. The above images are representative of PCNA staining seen in the middle aged liver, aged liver, and abnormal growths analyzed by PCNA immunohistochemistry. PCNA staining intensity and distribution in the abnormal growths collected from the Dox-induced aged mice transgenic for Tubedown overexpression was compared to that seen in liver tissues collected from both middle-aged (6 months old) and aged (17.5 months old) control mice.

Blood vessels are indicated by arrows. Positive PCNA staining is indicated by pink nuclear staining.

Compared to the middle aged liver (A) and aged liver (B), there was significantly more intense and altered distribution of PCNA staining present in the liver growth collected from a Dox-induced aged mouse transgenic for Tubedown overexpression (C). PCNA staining was quantified in Figure 11.

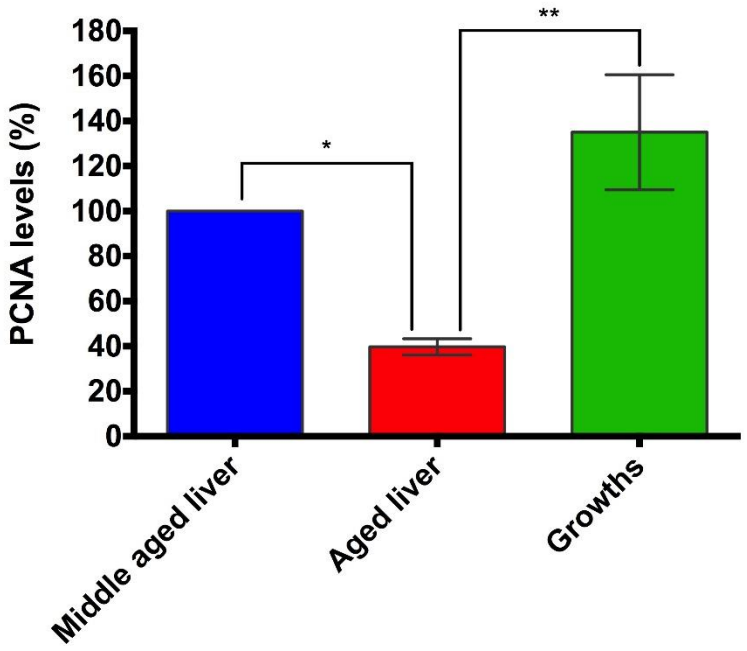

Figure 11. Abnormal cell proliferation in the abnormal tissue growths collected from the livers and peritoneum of Dox-induced aged mice transgenic for Tubedown overexpression suggested by PCNA immunohistochemistry.

Staining for the proliferation marker proliferative cell nuclear antigen (PCNA) was conducted on control liver tissues in comparison to our abnormal growths collected from the livers and peritoneum of Dox-induced *HHrtTAXK-TRE/HA-TBDN* aged mice. PCNA staining intensity in the abnormal growths collected from Dox-induced aged mice transgenic for Tubedown overexpression were compared to PCNA staining seen in control liver tissue collected from both middle-aged (6 months old) and aged (17.5 months old) control mice. Average PCNA levels $\pm$ SEM of at least 6 tissue sections. *ANOVA*; *, $P < 0.05$; **, $P < 0.005$.

The abnormal growths collected from the liver and peritoneum expressed significantly more PCNA than the aged liver tissue collected from control *HHrtTAXK* mice (*ANOVA*, $P < 0.005$).

3.2.4 Tubedown expression and tumor growth in aged mice.

I analyzed three abnormal growths detected from Dox-induced aged mice transgenic for TBDN overexpression, two abnormal growths collected from liver tissue and one peritoneal 'gut' growth. The abnormal histological characteristics and proliferation, paired with the overexpression of TBDN in the cells and blood vessels, these abnormal growths are likely tumor tissues. TBDN staining in the liver tumors and peritoneal tumor was significantly more intense in both the tumor cells and blood vessels when compared to normal control tissues (Figures 7-8). TBDN is overexpressed in these liver tumors and peritoneal tumor collected from three different Dox-induced aged mice transgenic for TBDN overexpression (Figure 9).

TBDN is overexpressed in the cells and blood vessels of the liver and peritoneal tumors collected from Dox-induced aged mice transgenic for TBDN overexpression. These are tumor types only found in the cohort of Dox-induced aged mice transgenic for TBDN overexpression, and not in any of our control aged mice not overexpressing TBDN under the inducible *Tie2* promoter. This suggests that TBDN overexpression may induce tumor formation in specific tissues under the control of the endothelial/mesenchymal *Tie2* promoter. Based on the results of our immunohistochemical analyses, I postulate that some tumor growth in aged mice is related to overexpression of TBDN, while other spontaneous age-related abnormal lung growths may not be directly related to TBDN levels.

3.2.5 p53 expression increases during aging in control mice, and p53 expression is suppressed in aged mice transgenic for Tubedown overexpression.

In connection with my *in vitro* data collected using Ewing's sarcoma EWS-96 cells, I wanted to investigate the effect of TBDN overexpression during aging on p53 expression. *In vitro*, I confirmed that knocking down TBDN expression resulted in a statistically significant increase in p53 expression in the Ewing's sarcoma EWS-96 cell line. I wanted to investigate this relationship *in vivo* with a mouse model in order to determine if overexpressing TBDN during aging in mice resulted in suppressed p53 expression in comparison to control aged mice.

It is known that p53 expression increases during aging in mouse tissues (Rufini et al. 2013). Therefore, we expected that p53 expression would increase during aging in our control mice.

I investigated the trend of p53 expression during aging in the *HHrtTAXK* control mouse cohort. I separated mice into three age groups: young (less than 6 months old); middle aged (7-14 months); and aged (greater than 15 months). p53 showed a stepwise increase in expression during normal aging in the liver tissue of *HHrtTAXK* control mice (Figure 12). Aged mice show higher levels of p53 expression in their liver tissue when compared to p53 levels found in the liver tissues of young mice (Figure 12B; young mice vs. aged mice: *ANOVA,* $P < 0.0001$).

I wanted to further investigate the effect of TBDN on the p53 pathway during aging by looking at the expression of p53 in Dox-induced aged mice transgenic for TBDN overexpression in comparison to *HHrtTAXK* control aged mice. Based on Western blot analysis of liver tissues, I found that Dox-induced aged mice transgenic for TBDN overexpression showed significantly lower p53 protein levels when compared to *HHrtTAXK* control aged mice (Figure 12B; *ANOVA*, $P < 0.005$).

Overall, p53 expression increases with aging in control mice; this increase in p53 expression seen with normal aging is interrupted by the induction of Tubedown overexpression during aging, as seen in the Dox-induced *HHrtTAXK-TRE/HA-TBDN* aged mice transgenic for Tubedown overexpression.

(A)

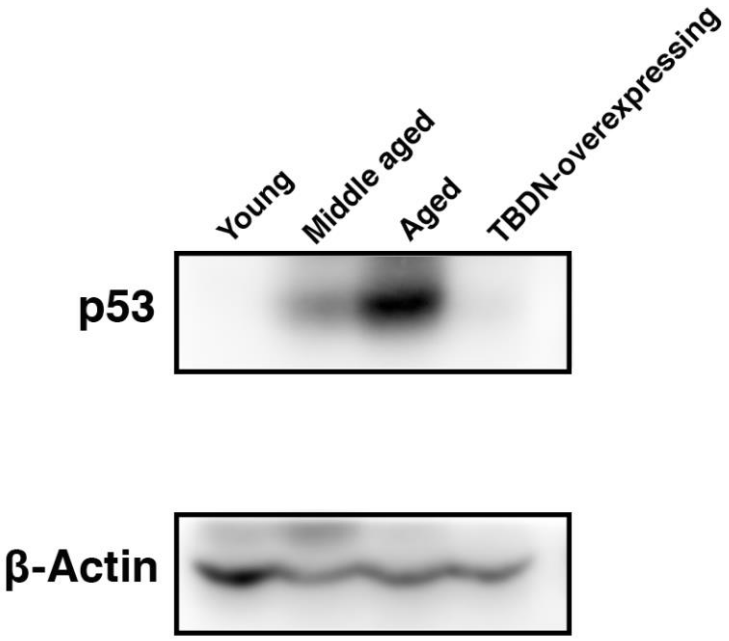
Young
Middle aged
Aged
TBDN-overexpressing
p53
β-Actin

(B)

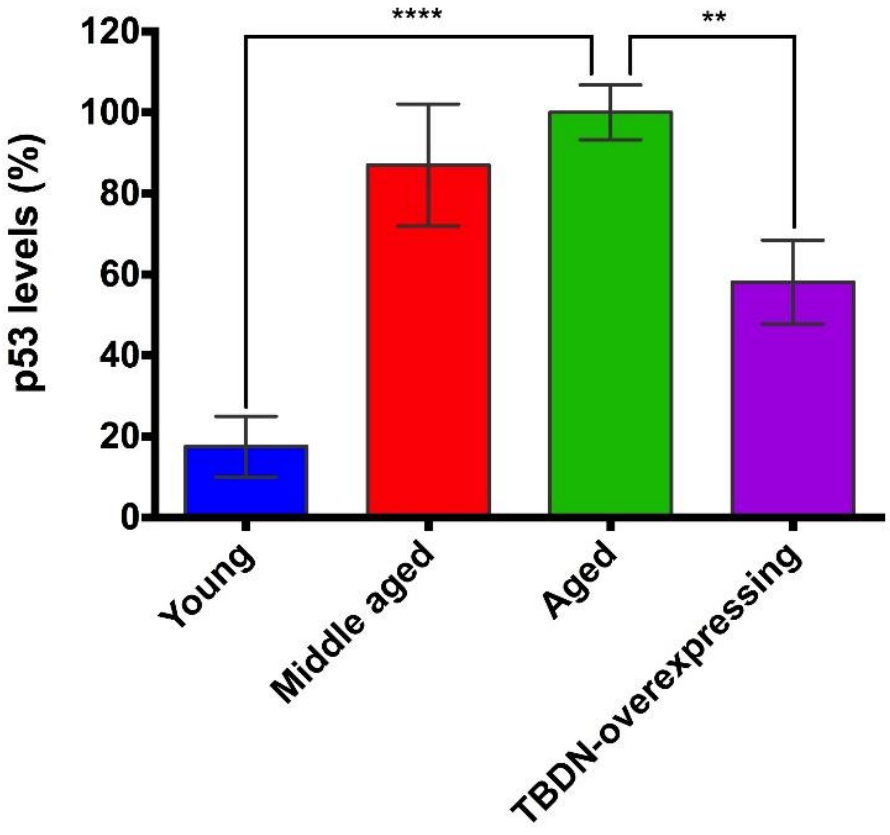
****
**
120
100
80
60
40
20
0
p53 levels (%)
Young
Middle aged
Aged
TBDN-overexpressing

Figure 12. p53 expression increases in control mice during aging, and is suppressed in Dox-induced aged mice transgenic for Tubedown overexpression.

p53 expression in the liver tissues of *HHrtTAXK* mice (young, middle aged, and aged) and Dox-induced aged mice transgenic for Tubedown overexpression (TBDN-overexpressing) were analyzed by Western blot. **(A)** Representative Western blot; liver, 125 ug protein. **(B)** Average p53 levels $\pm$ SEM of at least 3 specimens. *ANOVA*; *, $P < 0.05$; **, $P < 0.005$; ***, $P < 0.0005$; ****, $P < 0.0001$.

p53 levels in the liver tissues of aged mice (green; 17.5 months old) were significantly higher than the p53 levels seen in young mice (blue; < 6 months old) (*ANOVA,* $P < 0.0001$). p53 levels in the Dox-induced aged mice transgenic for Tubedown overexpression (purple) were significantly lower than p53 levels seen in aged mice (green) (*ANOVA,* $P < 0.005$).

3.2.6 Tubedown is overexpressed in the tumors of mice overexpressing Tubedown and is involved in the regulation of p53 expression during aging.

Combined, these data suggest a functional relationship between Tubedown and p53 during aging and in cancer. *In vitro*, we were able to confirm that knocking down Tubedown expression in an Ewing's sarcoma cell line, known to express the high levels of Tubedown characteristic of Ewing's sarcoma tumors, resulted in the upregulation of p53 expression (Figure 3) and the suppression of tumor cell growth (Figure 5). I confirmed that Tubedown was overexpressed in the blood vessels and cells of two liver tumors and one peritoneal tumor collected from Dox-induced aged mice transgenic for Tubedown overexpression (Figures 7-9). I showed that these tumor tissues showed abnormal cell proliferation levels and distribution, in reference to the high levels and abnormal distribution of PCNA expression seen in the tumor tissue in comparison to control aged tissues (Figures 10-11). This increased cell proliferation in aging tissues, in combination with the abnormal histological characteristics, confirms that these tissues are likely tumors.

In summation, the relationship between Tubedown expression and p53 expression during aging was confirmed by Western blot. I determined that p53 expression increased during aging in control mice, with aged mice (greater than 16 months old) showing significantly higher p53 expression than young mice (less than 6 months old) (Figure 12; *ANOVA,* $P < 0.0001$). Dox-induced aged mice transgenic for Tubedown overexpression showed significantly reduced p53 expression in comparison to control aged mice (Figure 12; *ANOVA,* $P < 0.005$). This suggested that Tubedown overexpression during aging suppressed the increase in p53 expression normally seen in aging tissues. These data connected the functional relationship between Tubedown overexpression in cancer and during aging, and a corresponding reduction in the protein expression levels of the tumor suppressor p53.

Chapter 4 Discussion

N^{α}-terminal acetylation is a type of co-translational modification known to influence protein stability, localization, and protein-protein interactions (Arnesen et al. 2009, Gromyko et al. 2010). NatA is one of the six eukaryotic N^{α}-terminal acetyltransferases, and is structurally composed of two subunits: the catalytic subunit Arrest-defective-1 protein (ARD1) and the regulatory subunit Tubedown (TBDN). The binding of ARD1 with TBDN induces an activating conformational change in the protein structure, which opens up the active site of ARD1 and allows the NatA complex to acetylate substrate polypeptide chains at specific N-terminal residues (Liszczak et al. 2013). NatA has thousands of potential substrates which have been identified by mass spectrometry (Arnesen et al. 2009, Gromyko et al. 2010). Being that acetyltransferase activity has been implicated in regulating the maintenance of normal cell growth and differentiation (Arnesen et al. 2009), it has been suggested that acetyltransferases and their subunits could be potential targets for cancer therapies (Gromyko et al. 2010).

TBDN, now known to be the regulatory subunit of NatA, was discovered as a developmentally regulated protein (Arnesen et al. 2009, Gendron et al. 2000, Gromyko et al. 2010). It is known that TBDN expression is tightly regulated and highly expressed during development specifically in neuroectodermal and mesenchymal lineages (Gendron et al. 2000, Sugiura et al. 2003). TBDN expression is highly regulated in developing neuronal cells and blood vessels during embryogenesis (Gendron et al. 2000). It has been shown that TBDN is highly expressed in certain childhood cancers, specifically neuroblastoma, osteosarcoma, and Ewing's sarcoma (EWS) (Kalvik and Arnesen 2013, Martin et al. 2007, Starheim and Gromyko et al. 2009; Dr. H. Paradis, personal communication). Using stable transfectant clones for an antisense fragment of TBDN cDNA, it has been established in the Paradis/Gendron lab (Dr. H.

Paradis, personal communication) that TBDN is necessary for the growth of the Ewing's sarcoma EWS-96 cell line, possibly via regulation of the p53 tumor suppressor pathway (Dr. H. Paradis, unpublished). I wanted to confirm these observations by looking at the effect of TBDN knockdown on p53 levels in a transient siRNA transfection of the Ewing's sarcoma EWS-96 cell line *in vitro*. My data indicated that TBDN may be a good candidate for developing a targeted therapy in the treatment of Ewing's sarcoma.

The current treatment for Ewing's sarcoma involves cytotoxic drug chemotherapy followed by radiation and surgery (Arndt and Crist 1999, Biswas and Bakhshi 2016, Palumbo and Zwerdling 1999, Yu et al. 2016). These treatments present a risk of relapse, in both metastatic and localized disease, and have variable survival rates. Patients with metastatic Ewing's sarcoma have a survival rate of 20-30%, while patients with localized disease show 70-80% survival (Fergurson and Turner 2018, Fizazi et al. 1998, West 2000). The treatments available for Ewing's sarcoma need to be improved in order to increase survival rates and prevent disease relapse. In the present study, I examined the role of TBDN in Ewing's sarcoma and during aging in mice, specifically in relation to the p53 tumor suppressor pathway, in order to better understand the role of N^{α}-terminal acetyltransferases in cancer and aging. My data suggested that TBDN offers a new potential target for the development of new treatments against Ewing's sarcoma.

Recent unpublished data in the Paradis/Gendron lab suggests that TBDN may be involved in regulating tumor cell growth and differentiation processes via regulation of the p53 tumor suppressor pathway (Dr. H. Paradis, personal communication). p53 is known to be lost or mutated in 55% of tumors, while p53 signaling pathway members are mutated or deregulated in the remaining percentage of tumors (Barone et al. 2014, Nostrand et al. 2017, Reed and Quelle

2015). The dysregulation of the normal tumor suppressive functions of p53 will lead to tumor progression. p53 activity is modulated by a number of post-translational modifications, including acetylation. The acetylation of p53 achieves the stabilization and subsequent accumulation of p53 in the cell; acetylations at specific lysine (Lys) residues of the p53 protein are required for the activation of tumor suppression by p53 in the cell (Brooks and Gu 2011, Dai and Gu 2010, Reed and Quelle 2015, Tang et al. 2008). When the normal acetylation pattern of p53 is disrupted, the normal tumor suppressive functions of p53 are inhibited (Reed and Quelle 2015). Alterations to normal p53 acetylation will result in the loss of its normal tumor suppressive functions. As NatA is an N^{α}-terminal acetyltransferase with thousands of potential substrates, I postulated that the NatA complex, or its subunits ARD1 or TBDN, were involved in the regulation of the p53 pathway.

In the present functional study, I examined the role of TBDN in the Ewing's sarcoma EWS-96 cell line and during aging in mice, specifically in relation to the p53 tumor suppressor pathway, in order to better understand the role of N^{α}-terminal acetyltransferases in cancer and aging.

I examined the role of TBDN in p53 tumor suppression in Ewing's sarcoma during aging using a transient siRNA knockdown approach. I used the human-derived cell line EWS-96, developed by Dr. Theodore Zwerdling from the tumor of an Ewing's sarcoma patient. Ewing's sarcoma EWS-96 cells with knocked down TBDN or ARD1 expression showed upregulation of p53 expression and suppressed cell growth when compared to controls (TBDN knockdown, Figures 3 and 5; ARD1 knockdown, Figures 4 and 6). My data suggest a role for TBDN and ARD1, either in complex as the NatA complex or as individual subunits, in regulating p53 tumor suppression and tumor cell proliferation in Ewing's sarcoma. It is known that TBDN is highly

expressed and tightly regulated during embryogenesis, and the regulation of TBDN expression is particularly important in the differentiation of vascular and neural lineages (Gendron et al. 2000, Gendron et al. 2001, Sugiura et al. 2003). TBDN is only expressed in a select few tissues of the adult, followed by downregulation in expression during normal aging as demonstrated in the retinal vasculature (Gendron et al. 2000, Gendron et al. 2010, Paradis et al. 2002). ARD1 is widely expressed, and its expression – either suppressed levels or overexpression – has been implicated in varying capacities in different types of cancer, with ARD1 shown to function as a tumor suppressor or an oncoprotein in different types of cancer cells (Kalvik and Arnesen 2013). The functional role of ARD1 in cancer pathogenesis has yet to be fully elucidated. Together, ARD1 and TBDN form the NatA complex. In studies conducted thus far by numerous groups, it has been shown that high levels of TBDN expression are seen in numerous types of cancers, including the adolescent/childhood cancers Ewing's sarcoma, osteosarcoma, and neuroblastoma (Martin et al. 2007, Starheim and Gromyko et al. 2009, Kalvik and Arnesen 2013; Dr. H. Paradis, personal communication). We have demonstrated that the knockdown of TBDN expression in the Ewing's sarcoma EWS-96 cell line induced p53 levels and suppressed tumor cell proliferation (Figures 3 and 5). My data indicated that the knockdown of TBDN expression in Ewing's sarcoma cells may offer a new therapeutic strategy in the management and treatment of Ewing's sarcoma tumors.

In Ewing's sarcoma, ARD1 and TBDN may be required – in complex as the N^{α}-terminal acetyltransferase NatA or as individual subunits – for the downregulation of p53 expression and the promotion of cancer cell proliferation; this may facilitate tumor progression. It is known that 90% of Ewing's sarcoma tumors maintain wildtype p53 (Barone et al. 2014). Since wildtype p53 remains intact in many Ewing's sarcoma tumors, a specific mechanism by which Ewing's

sarcoma cancer cells overcome normal host tumor suppression is yet to be elucidated. High levels of TBDN and ARD1 expression and/or the NatA N^{α}-terminal acetylation pathway could provide the mechanistic link between downregulated p53 tumor suppression and the growth and advancement of Ewing's sarcoma family tumors. In the present study, we found that suppressing TBDN expression in an Ewing's sarcoma cell line resulted in an increase in p53 levels (Figure 3). This suggests a possible role for TBDN expression in the mechanism of the downregulation of p53 tumor suppression in Ewing's sarcoma.

There are multiple targets of NatA identified by mass spectrometry which are involved in the regulation of the p53 pathway or are known to interact with p53 pathway components or regulators in some manner (Myklebust et al. 2015, Reed and Quelle 2015). I have identified several factors which may provide a mechanistic link between TBDN overexpression and the downregulation of p53 tumor suppression. Based on data published by Myklebust et al. (2015), we conducted a comparison of known NatA targets (Myklebust et al. 2015) and known p53 pathway regulators (Reed and Quelle 2015) in order to determine a potential mechanistic link between NatA and the p53 pathway. The MYST family of histone acetyltransferases, specifically Tip60, MOF, and MOZ, are possible targets of NatA and are known to be involved in enhancing p53 functions by acetyltransferase activity (Reed and Quelle 2015). Sirtuins (SIRT), another family of histone deacetylases, are suggested targets of acetylation by the NatA complex (Reed and Quelle 2015). It is known that SIRT family proteins are a family of histone deacetylases known to regulate many cellular metabolic functions, including DNA repair, apoptosis, and the cell cycle (Watroba and Szukiewicz 2016). More specifically, it is known that sirtuins are negative regulators of p53; this could provide a possible link between the high levels of TBDN expression characteristic of Ewing's sarcoma and the downregulation of p53 tumor

suppression leading to tumor progression (Watroba and Szukiewicz 2016). Src kinase is another potential target of NatA, and is known to suppress p53-mediated apoptosis by mediating the phosphorylation of p53 phosphorylase HIPK2 (Myklebust et al. 2015, Polonio-Vallon et al. 2014). Another candidate is securin (Sec1), a possible target of NatA identified by mass spectrometry and a known inhibitor of p53 in the induction of p53-dependent apoptosis (Bernal et al. 2002, Reed and Quelle 2015). Based on the mass spectrometry analysis used to identify NatA targets involved in p53 pathway regulation (Myklebust et al. 2015, Reed and Quelle 2015), there are many potential mechanistic and functional links between TBDN and ARD1, and the regulation of p53 tumor suppression.

Also in the present study, I examined the role of TBDN in the p53 tumor suppressor pathway during aging in mice. These mice overexpressed TBDN under the inducible endothelial-/mesenchymal- specific *Tie2* promoter. The overexpression of TBDN in the mice has been confirmed previously by Western blot for the non-endogenous HA-tagged TBDN protein (Dr. H. Paradis, personal communication). Our control groups included mice induced and non-induced with doxycycline (Dox); these mice did not overexpress TBDN in endothelial and mesenchymal tissues under the *Tie2* promoter.

Dox-induced aged mice transgenic for TBDN overexpression show increased incidence of abnormal tissue growths when compared to control aged mice (Dr. H. Paradis, personal communication). Abnormal lung growths in aged mice of the control groups, *HHrtTAXK* control aged mice and non-induced aged mice transgenic for TBDN overexpression, as well as in the Dox-induced aged mice overexpressing TBDN, were observed (Table 1; Dr. H. Paradis, personal communication). Abnormal growths have been isolated to the lung tissue of aged control mice. In the cohort of Dox-induced aged mice transgenic for TBDN overexpression, specific abnormal

growths in the liver, peritoneum, pancreas, uterine tissue, brain, kidney, and epididymis have been observed (Table 1; Dr. H. Paradis, personal communication). Abnormal growths formed only in aged mice; no abnormal growths have been found during middle age (Dr. H. Paradis, personal communication).

This formation of abnormal growths in specific tissues is associated with increased TBDN expression. It has been confirmed by Western blot that TBDN overexpression was achieved in the Dox-induced aged mice transgenic for TBDN overexpression under the inducible endothelial/mesenchymal *Tie2* promoter (Dr. H. Paradis, personal communication). Western blot confirmed the expression of HA-tagged TBDN, the non-endogenous TBDN isoform, in the Dox-induced aged mice transgenic for TBDN overexpression (Dr. H. Paradis, personal communication). The expression of HA-tagged TBDN, the non-endogenous isoform of TBDN, was not seen in the control mice (Dr. H. Paradis, personal communication). This confirms that TBDN overexpression was achieved in Dox-induced aged mice transgenic for TBDN overexpression, and not in the control mice. I examined the expression of TBDN in the cells and blood vessels of these abnormal growths, and verified that these abnormal growths were indeed tumors.

I focused my study on the examination of three abnormal growths collected from the livers and peritoneum of three separate Dox-induced aged mice transgenic for TBDN overexpression. I selected these for our analysis in order to ensure that I was analyzing tumors specific to the cohort of TBDN-overexpressing mice.

I found that TBDN was overexpressed in the tumor cells and tumor blood vessels of the two liver tumors and one peritoneal 'gut' tumor collected from Dox-induced aged mice transgenic for TBDN overexpression (Figures 7-9). In middle aged spleen, faint TBDN staining

was isolated to the blood vessels (Figure 8E). In the middle aged liver and aged liver tissue, faint TBDN staining was also isolated to the blood vessels; there was a slight increase in TBDN expression in the blood vessels of aged liver tissue when compared to middle aged liver (Figure 7D-E and Figure 8F-G). I observed TBDN overexpression in the tumor cells and tumor blood vessels of both liver tumors and the peritoneal tumor that I analyzed, in comparison to middle aged and aged control tissues (Figure 7F and Figure 8H). There was significantly higher intensity TBDN staining seen in the cells and blood vessels of the two liver tumors and one peritoneal 'gut' tumor, when compared to middle aged liver, middle aged spleen, and aged liver tissues (Figure 9; *ANOVA*, $P < 0.0001$). The abnormal liver and peritoneal 'gut' growths, found to be overexpressing TBDN in the tumor cells themselves as well as in the blood vessels of the tumor, were found to occur in these tissue types only in Dox-induced aged mice transgenic for TBDN overexpression and not in control aged mice. These data provided evidence that TBDN overexpression induced the formation of these tumors specifically in the Dox-induced aged mice overexpressing TBDN under the endothelial-/mesenchymal- specific *Tie2* promoter.

I confirmed by immunohistochemistry for PCNA that the cells in these abnormal growths collected from the livers and peritoneal tissue of three Dox-induced aged mice transgenic for TBDN overexpression also showed abnormal levels and distribution of cell proliferation when compared to control middle aged and aged tissues (Figures 10-11). The liver and peritoneal growths collected from our cohort of Dox-induced aged mice transgenic for TBDN overexpression were overexpressing proliferating cell nuclear antigen (PCNA) in comparison to control liver tissue from aged mice (Figure 11; *ANOVA*, $P < 0.005$ for all 3 tumors). I observed high levels of PCNA expression in the abnormal growth tissue collected from Dox-induced aged

mice transgenic for TBDN overexpression, indicating that these tissues were proliferating abnormally in comparison to control aged tissue.

During aging, I observed an increase in the area of liver tissue that was occupied by presumably fatty deposits; these appeared as empty 'bubbles' of space on the tissue sections affixed to slides for analysis. As I observed some areas of 'fatty liver' in our control aged mice, I wanted to confirm that the cells in our abnormal liver growths sections collected from Dox-induced aged mice transgenic for TBDN overexpression were exhibiting a cancer-cell characteristics in their proteome in addition to their abnormal histological characteristics. This would confirm to us that these abnormal growths were tumors, and that these tumors were likely induced by TBDN overexpression in our Dox-induced aged mice transgenic for TBDN overexpression under the endothelial/mesenchymal *Tie2* promoter. I observed a statistically significant increase in PCNA expression in the abnormal growths when compared to control aged mice (Figure 11; *ANOVA*, $P < 0.005$). Interestingly, I also observed changes in the distribution of cells expressing PCNA (Figure 10). In middle aged liver tissue, I saw a uniform distribution of cells expressing relatively equal levels of PCNA throughout the tissue (Figure 10A). In aged liver tissue, I observed PCNA expression sharply decrease in intensity, but with no changes in the uniform distribution of the staining (Figure 10B). In the abnormal liver and peritoneal growths, I saw high levels of PCNA expression in specific regions of the tissue indicative of non-uniform and abnormal cell proliferation (Figure 10C). The high levels and abnormal distribution of PCNA expression seen in the peritoneal and liver growth sections in comparison to control aged liver tissue suggested that these cells were proliferating abnormally. This characteristic supports the results of the histological analysis and confirms that these are tumors and not just fatty deposits presumably observed in normal aging liver tissues.

Based on my data, some tumor growth in aged mice is related to overexpression of TBDN, while other spontaneous age-related lung growths may not be directly related to TBDN levels. There are two possible mechanisms to explain the formation of tumors in multiple different tissues in the Dox-induced aged mice transgenic for TBDN overexpression. We know that the *Tie2* promoter is specific to mesenchymal and endothelial tissues. Tumors may be driven by overexpression of TBDN in the endothelium (ie. vasculature) directly through the induction of the *Tie2* endothelial promoter; or, tumors may be derived from a *Tie2*-related pathway in non-endothelial cells. The development of abnormal growths under the induction of the *Tie2* promoter in tissues not directly derived from endothelium, including tissues known to be of mesenchymal origin has been observed (Dr. H. Paradis, personal communication). Tie2 expression is detected as the first endothelial cells arise, remains positive in endothelial cells throughout development, and is detectable in virtually all endothelial cells of adult tissues (Kisanuki et al. 2001). It is known that the *Tie2* promoter is active in the endothelium and in mesenchyme, specifically in mesenchymal progenitor cells (Sato et al. 1995). This could be the driving force behind tumor formation in non-endothelial tissues induced by TBDN overexpression under the *Tie2* promoter, as this promoter is known to be active in mesenchymal progenitor cells. The mesenchymal lineage gives rise to numerous tissues, including connective tissues, endothelium, dendritic cells, fibroblasts, muscle, and immune cell lineages (Guan and Chen 2013). The diversity of the *Tie2* promoter activity in tissues under the endothelial and mesenchymal lineages could provide an explanation for the incidence of tumors in multiple tissues during aging that we see in Dox-induced aged mice transgenic for TBDN overexpression.

Since TBDN is overexpressed under the *Tie2* promoter in the endothelial and mesenchymal lineage, this could be the driving force behind tumor formation in various tissues

induced by TBDN overexpression under the *Tie2* promoter. The tissues where tumors appear to be induced in our Dox-induced aged mice transgenic for TBDN overexpression are of diverse embryonic origins, including ectodermal-derived liver, peritoneal, and pancreas, and mesodermal-derived brain, kidney, uterine, and epididymis (Dyer and Patterson 2010, Harvey and Oliver 2004). The *Tie2* promoter is known to be active in mesenchymal and endothelial tissues (Sato et al. 1995). We see the induction of tumors in organs known to be made up of tissues of mesenchymal origin in Dox-induced aged mice transgenic for TBDN overexpression. Tumor types found in both the control mice not transgenic for TBDN overexpression and the TBDN-overexpressing mice (ie. lung tumors) may form spontaneously with age via an alternate mechanism not directly related to TBDN overexpression in the endothelium and mesenchyme under the *Tie2* promoter. Tumors found exclusively in the Dox-induced aged mice overexpressing TBDN under the *Tie2* promoter may be induced directly by the overexpression of TBDN in the endothelium and in tissues of mesenchymal origin.

Based on the trend I observed in the Ewing's sarcoma EWS-96 cell line, suggesting that knocked down TBDN expression induced p53 expression, I postulated that TBDN overexpression in the vasculature and mesenchymal tissues of Dox-induced aged mice transgenic for TBDN overexpression would be accompanied by suppressed p53 expression.

I expected to see an increase in expression of p53 during normal aging, as aging cells are under more cellular stress, resulting in the robust activation of the p53 protein and performance of its subsequent tumor suppressive responses (Rufini et al. 2013). I postulated that increased TBDN expression in mice during aging may correspond to a decrease in p53 expression; this would explain the growth of the tumor and the increased tumor burden experienced by the host.

I wanted to find the correlation between TBDN levels and p53 expression during aging in the Paradis/Gendron aged mouse model overexpressing TBDN under the inducible *Tie2* endothelial/mesenchymal promoter (derived by Dr. H. Paradis). Specifically, I wanted to investigate the trend in p53 expression during aging in the control mice and the effects of TBDN overexpression during aging on p53 levels in the Dox-induced aged mice transgenic for TBDN overexpression.

Based on the data I have collected with the Ewing's sarcoma EWS-96 cell line and my histological and immunohistochemical analyses of tumors collected from Dox-induced aged mice transgenic for TBDN overexpression, there are three possible scenarios which I have postulated that define the potential role of TBDN in regulating p53 tumor suppression. Firstly, TBDN overexpression in mice during aging may be independent of tumor formation. The data collected thus far by the Paradis/Gendron lab indicate that there is a correlation between TBDN overexpression in mice as they age and an increase in tumor incidence; therefore, this explanation seems less likely. Secondly, TBDN overexpression may directly induce tumor formation in specific tissues under the endothelial/mesenchymal *Tie2* promoter. The mesenchymal lineage gives rise to numerous tissues, including connective tissues, endothelium, dendritic cells, fibroblasts, muscle, and immune cell lineages (Guan and Chen 2013). This could provide an explanation for the incidence of tumors in multiple tissues that is seen during aging in Dox-induced aged mice transgenic for TBDN overexpression, as the induction of the *Tie2* promoter is active in mesenchymal lineages. Thirdly, TBDN overexpression may not need to persist to induce tumor formation in aged mice. The overexpression of TBDN in mice during aging is induced for 14 weeks using doxycycline administered in the diet; however, the overexpression of TBDN may not persist over the 14 week period. Metabolic, genomic, and/or

biochemical changes induced by TBDN overexpression could be responsible for tumorigenesis observable at a later time point in these same mice.

I found that p53 expression increased during aging in the liver tissue of *HHrtTAXK* control mice; there was a statistically significant increase in p53 protein levels in the liver tissues of aged mice (17.5 months old) when compared to p53 levels in young mice (< 6 months old) (Figure 12; *ANOVA*, $P < 0.0001$). In comparing p53 expression in *HHrtTAXK* control aged mice to Dox-induced aged mice transgenic for TBDN overexpression, I observed a statistically significant decrease in p53 expression in the liver tissue of the Dox-induced aged mice transgenic for TBDN overexpression (Figure 12; *ANOVA*, $P < 0.005$). Overall, the increase in p53 expression seen during normal aging is interrupted by the induction of TBDN overexpression during aging, as seen in the Dox-induced aged mice transgenic for TBDN overexpression. This bolsters my suggested functional relationship between TBDN overexpression seen in certain cancers and the deregulation of normal p53 protein expression. The net result of TBDN overexpression in a tumor would be disrupted p53 tumor suppression, and progression of the tumor.

All of my *in vitro* and *in vivo* data supported the same common functional relationship between TBDN and the p53 pathway. There was an inverse relationship seen between TBDN and p53 protein levels. With a knockdown of TBDN expression in our Ewing's sarcoma EWS-96 cell line *in vitro*, I observed a statistically significant upregulation of p53 expression and the suppression of tumor cell proliferation (Figures 3 and 5). In my *in vivo* study looking at the effects of TBDN overexpression under the endothelial-/mesenchymal- specific *Tie2* promoter during aging in the mouse model, I concluded that overexpressing TBDN resulted in the suppression of p53 protein expression in Dox-induced aged mice transgenic for TBDN

overexpression in comparison to *HHrtTAXK* control aged mice (Figure 12). I observed that TBDN is overexpressed in the cells and blood vessels of tumors collected from the livers and peritoneum of Dox-induced aged mice transgenic for TBDN overexpression (Figures 7-9).

I have identified a functional relationship between TBDN expression and the p53 tumor suppressor pathway. *In vitro*, when TBDN expression was knocked down in Ewing's sarcoma EWS-96 cells I observed a statistically significant upregulation in p53 expression and the suppression of tumor cell proliferation. *In vivo*, when TBDN was overexpressed in mice during aging under the endothelial-/mesenchymal- specific *Tie2* promoter, it was noted that there was increased tumor incidence in tissues unique to mice overexpressing TBDN and not seen in control aged mice not overexpressing TBDN in endothelial and mesenchymal tissues (Dr. H. Paradis, personal communication). Further, these tumors collected from Dox-induced aged mice transgenic for TBDN overexpression showed higher intensity TBDN staining in their cells and blood vessels when compared to the middle aged and aged liver and spleen tissues of *HHrtTAXK* control aged mice. Additionally, I confirmed that the stepwise increase in p53 expression during aging in the liver tissues of *HHrtTAXK* control aged mice was interrupted in Dox-induced aged mice overexpressing TBDN under the endothelial/mesenchymal *Tie2* promoter. When TBDN was overexpressed during aging, the normal increase in p53 expression seen in aged liver tissue was reversed; I saw much lower p53 protein levels in the liver tissue of Dox-induced aged mice transgenic for TBDN overexpression when compared to *HHrtTAXK* control aged mice. All of my data support a link between the upregulation of TBDN expression and suppressed p53 expression during aging, and subsequent tumor development.

4.1 Proposed mechanism for Tubedown regulation of the p53 tumor suppressor pathway

Based on my *in vitro* analysis using the Ewing's sarcoma EWS-96 cell line and *in vivo* analysis using an inducible mouse model transgenic for TBDN overexpression, I have postulated a mechanism by which TBDN is involved in the regulation of the p53 pathway (Figure 13). TBDN is the regulatory subunit of the N^{α}-terminal acetyltransferase complex NatA, and is able to modulate the ability of ARD1, the catalytic subunit, to acetylate NatA substrates. TBDN may regulate p53 levels by controlling the acetylation of a regulator or component of the p53 pathway. Therefore, I suggest that TBDN regulates the p53 pathway via control of the NatA acetylation of a regulator of p53 (Figure 13).

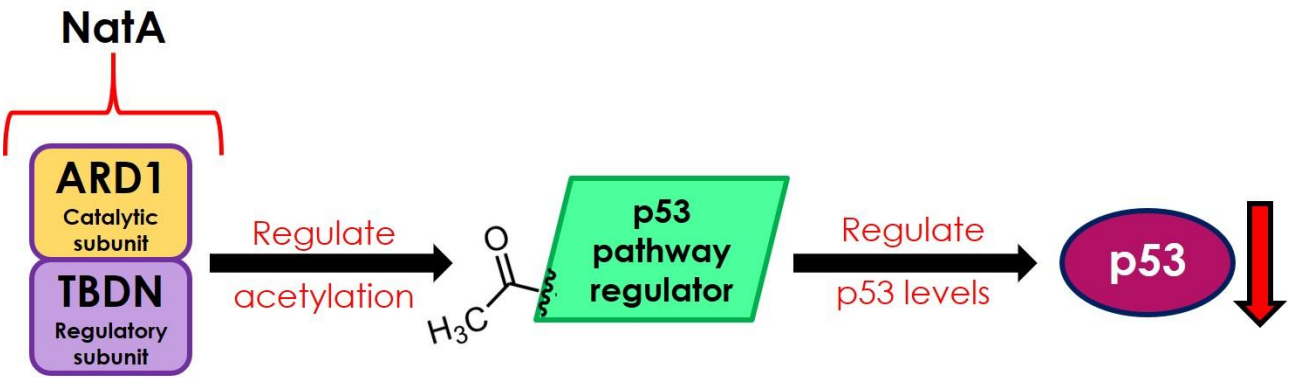

Figure 13. Schematic diagram showing a possible mechanism by which Tubedown is involved in the regulation of the p53 pathway.

Tubedown regulates the p53 pathway via control of the NatA acetylation of a regulator of the p53 tumor suppression pathway. Tubedown, the regulatory subunit of the N^{α}-terminal acetyltransferase complex NatA, is involved in the regulation of the p53 tumor suppression pathway. ARD1 is the catalytic subunit of the NatA complex. Tubedown is able to modulate the catalytic activity of NatA. This regulatory function may allow Tubedown to regulate the acetylation of a p53 pathway regulator, and in turn modulate the levels of p53 present in the cell. With the overexpression of Tubedown there is a corresponding decrease in p53 expression.

Chapter 5 Conclusions

In Ewing's sarcoma (EWS), wildtype p53 remains intact in approximately 90% of tumors (Barone et al. 2014), suggesting that p53-mediated tumor suppression is deregulated by an indirect mechanism. Based on recent unpublished data collected in the Paradis/Gendron lab, it has been shown that TBDN is highly expressed in the Ewing's sarcoma EWS-96 cell line (Dr. H. Paradis, personal communication). The Paradis/Gendron lab has shown that TBDN is necessary for the growth of EWS cells *in vitro* and tumor xenografts in mice, possibly via regulation of differentiation processes and p53 tumor suppression (Dr. H. Paradis, unpublished). This study examined the effects of knocked down TBDN expression in Ewing's sarcoma cells, in relation to cell proliferation and p53 tumor suppression.

In knocking down TBDN expression, we observed an upregulation of the expression of the tumor suppressor p53 and the suppression of cell proliferation. Further, the knockdown of the catalytic subunit of the NatA complex, ARD1, also resulted in the upregulation of p53 expression and similar suppression of cell proliferation. Results show that the N^{α}-terminal acetyltransferase NatA, either as a complex or as its subunits TBDN and/or ARD1, is involved in the regulation of p53 tumor suppression and cell growth in Ewing's sarcoma cells.

We also wanted to examine the effects of TBDN overexpression in mice during aging; we accomplished this using a bi-transgenic aged mouse model under the control of the inducible endothelial/mesenchymal *Tie2* promoter (derived by Dr. H. Paradis).

The overexpression of TBDN during aging in Dox-induced mice transgenic for TBDN overexpression has been shown to result in the development of tissue specific tumors that are not observed in control aged mice (Dr. H. Paradis, personal communication). I analyzed three

tumors collected from Dox-induced aged mice transgenic for TBDN overexpression: two liver tumors and one peritoneal tumor. I found that TBDN was overexpressed in the tumor cells and tumor blood vessels of the liver tumors and peritoneal tumor collected from three Dox-induced aged mice transgenic for TBDN overexpression. Immunohistochemical analysis of tumor and control tissues suggested that tumor growth is related to the overexpression of TBDN in the Dox-induced aged mice transgenic for TBDN overexpression.

Based on the trends seen in my *in vitro* analysis of the Ewing's sarcoma EWS-96 cell line, where a knockdown of TBDN expression corresponded to an upregulation in p53 expression, I examined p53 expression *in vivo* using the inducible mouse model transgenic for TBDN overexpression (derived by Dr. H. Paradis). I postulated that TBDN overexpression in the vasculature and mesenchymal tissues of Dox-induced aged mice transgenic for TBDN overexpression would be accompanied by suppressed p53 expression.

Based on analysis of liver tissues collected from *HHrtTAXK* control aged mice, p53 expression increased during aging. Young mice (aged 3-6 months) had significantly lower p53 levels when compared to aged mice (greater than 15 months old). When comparing the Dox-induced aged mice transgenic for TBDN overexpression to our control aged mice, I found that mice overexpressing TBDN had significantly lower p53 levels. This corresponds to my data collected *in vitro* using the Ewing's sarcoma EWS-96 cell line; there appears to be an inverse relationship between TBDN expression and p53 levels. Induction of TBDN overexpression in the aged mouse model transgenic for TBDN overexpression suppressed the levels of p53 present in the liver in relation to normal control aged mice.

TBDN offers a new potential target for the treatment of Ewing's sarcoma. Increased expression of TBDN is associated with tissue specific tumors in the aged mouse model. TBDN

overexpression in endothelial and mesenchymal tissues under the *Tie2* promoter may induce tumor formation in endothelial and mesenchymal-derived tissues in Dox-induced aged mice transgenic for TBDN overexpression. I found that the overexpression of TBDN during aging in the mouse model interrupted the normal increase in p53 expression in the liver tissues of aged mice. Together, these data suggest a functional link between the upregulation of TBDN expression and the suppression of p53 expression during aging. I suggest that TBDN regulates the NatA acetylation of a p53 pathway member or regulator, in turn modulating the tumor suppressive functions of p53. The overexpression of TBDN during aging suppresses p53 expression and may lead to increased incidence of cancer. Overall, gaining a better understanding of the role of N^{α}-terminal acetyltransferases in cancer and aging will lead to the identification of better targets for the design of new treatments for cancer.

Cancer is an increasingly common disease affecting all age groups in our world today. We know that mutations of the tumor suppressor p53 or dysregulation of the p53 pathway and regulators of the p53 pathway are implicated in a number of cancers, with 55% of tumors showing direct mutations to p53 and the remaining tumors showing deregulation of p53 tumor suppression (Barone et al. 2014, Nostrand et al. 2017, Reed and Quelle 2015). Increasing knowledge of the role of TBDN in the regulation of the p53 pathway will improve the understanding of N^{α}-terminal acetyltransferases in cancer and aging.

5.1 Future directions

Future research is required to determine the exact mechanism by which TBDN regulates the p53 pathway. Isolating and confirming a specific interaction between TBDN and a p53 pathway regulator would finalize the mechanism of TBDN regulation of the tumor suppressor p53. Performing TBDN immunohistochemistry and PCNA immunohistochemistry on more tumors collected from Dox-induced aged mice transgenic for TBDN overexpression would provide further support for the data I have collected with the liver and peritoneal tumors. Examining the N^{α}-terminal acetylation status of p53 could assist in identifying the specifics of the interaction of NatA with a p53 pathway regulator. Possible future directions could also include immunohistochemical analysis of p53 expression in tumors collected from aged mice; this would further clarify the link between TBDN overexpression in mice during aging and the corresponding downregulation of p53 expression.

Chapter 6 References

Amann, G., Zoubek, A., Salzer-Kuntschik, M., Windhager, R., and Kovar, H. Relation of neurological marker expression and EWS gene fusion types in MIC2/CD99-positive tumors of the Ewing family. Hum. Pathol., 30: 1058-1064, 1999.

Arndt, C. A., and Crist, W. M. Common musculoskeletal tumors of childhood and adolescence. N. Engl. J. Med., 341: 342-352, 1999.

Arnesen, T., Gromyko, D., Kagabo, D., Betts, M. J., Starheim, K. K., Varhaug, J. E., Anderson, D., and Lillehaug, J. R. A novel human NatA N^{α}-terminal acetyltransferase complex: hNaa16p-hNaa10p (hNat2-hArd1). BMC Biochem, 10: 15, 2009.

Artigas, N., Gámez, B., Cubillos-Rojas, M., Sánchez-de Diego, C., Valer, J. A., Pons, G., Rosa, J. L., and Ventura, F. p53 inhibits SP7/Osterix activity in the transcriptional program of osteoblast differentiation. Cell Death Differ., 24: 2022-2031, 2017.

Barone, G., Tweddle, D. A., Shohet, J. M., Chesler, L., Moreno, L., Pearson A. D. J., and Maerken, T. V. MDM2-p53 interaction in paediatric solid tumors: preclinical rationale, biomarkers and resistance. Curr Drug Targets, 15: 114-123, 2014.

Bernal, J. A., Luna, R., Espina, A., Lazaro, I., Ramos-Morales, F., Romero, F., Arias, C., Silva, A., Tortolero, M., and Pintor-Toro, J. A. Human securing interacts with p53 and modulates p53-mediated transcriptional activity and apoptosis. Nature Genetics, 32: 306-311, 2002.

Biswas, B., and Bakhshi, S. Management of Ewing sarcoma family of tumors: current scenario and unmet need. World J Orthop, 7: 527-538, 2016.

Bologna-Molina, R., Mosqueda-Taylor, A., Molina-Frechero, N., Mori-Estevez, A., and Sánchez-Acuña, G. Comparison of the value of PCNA and Ki-67 as markers of cell proliferation in ameloblastic tumors. Med Oral Patol Oral Cir Bucal, 18: 174-179, 2013.

Bouleftour, W., Juignet, L., Bouet, G., et al. The role of the SIBLING, Bone Sialoprotein in skeletal biology - Contribution of mouse experimental genetics. Matrix Biol., 52-54: 60-77, 2016.

Brock, T. Protein acetylation: much more than histone acetylation. Cayman Chemicals, 2010.

Brooks, C. L., and Gu, W. The impact of acetylation and deacetylation on the p53 pathway. Protein Cell, 2: 456-462, 2011.

Dai, C., and Gu, W. p53 post-translational modification: deregulated in tumorigenesis. Trends Mol Med, 16: 528-536, 2010.

de Alava, E., and Gerald, W. L. Molecular biology of the Ewing's sarcoma/primitive neuroectodermal tumor family. J. Clin. Oncol., 18: 204-213, 2000.

Del Mare, S., Husanie, H., Iancu, O., Abu-Odeh, M., Evangelou, K., Lovat, F., Volinia, S., Gordon, J., Amir, G., Stein, J., Stein, G. S., Croce, C. M., Gorgoulis, V., Lian, J. B., Aqeilan, R. I. WWOX and p53 dysregulation synergize to drive the development of osteosarcoma. Cancer Res., 76: 6107-6117, 2016.

Donehower, L. A., Harvey, M., Slagle, B. L., McArthur, M. J., Montgomery, C. A., Butel, J. S., and Bradley, A. Mice deficient for p53 are developmentally normal but susceptible to spontaneous tumors. Nature, 356: 215-221, 1992.

Dyer, L. A. and Patterson, C. Development of the endothelium: an emphasis on heterogeneity. Semin. Thromb. Hemost., 36: 227-235, 2010.

Ferguson, J. L. and Turner, S. P. Bone cancer: diagnosis and treatment principles. Am Fam Physician, 98: 205-213, 2018.

Fizazi, K., Dohollou, N., Blay, J. Y., Guerin, S., Le Cesne, A., Andre, F., Pouillart, P., Tursz, T., and Nguyen, B. B. Ewing's family of tumors in adults: multivariate analysis of survival and long-term results of multimodality therapy in 182 patients. J. Clin. Oncol., 16: 3736-3743, 1998.

Gendron, R. L., Adams, L. C., and Paradis, H. Tubedown-1, a novel acetyltransferase associated with blood vessel development. Dev. Dyn., 218: 300-315, 2000.

Gendron, R. L., Good, W. V., Adams, L. C., and Paradis, H. Suppressed expression of Tubedown-1 in retinal neovascularization of proliferative diabetic retinopathy. IOVS, 42: 3000-3007, 2001.

Gendron, R. L., Laver, N. V., Good, W. V., Grossniklaus, H. E., Miskiewicz, E., Whelan, M. A., Walker, J., and Paradis, H. Loss of Tubedown expression as a contributing factor in the development of age-related retinopathy. Invest. Ophthalmol. Vis. Sci., 51: 5267-5277, 2010.

Gromyko, D., Arnesen, T., Ryningen, A., Varhaug, J. E., and Lillehaug, J. R. Depletion of the human N^{α}-terminal acetyltransferase A induces p53-dependent apoptosis and p53-independent growth inhibition. Int. J. Cancer, 127: 2777-2789, 2010.

Guan, J. and Chen, J. Mesenchymal stem cells in the tumor microenvironment. Biomed. Rep. 1(4): 517-521, 2013.

Harvey, N. L. and Oliver, G. Choose your fate: artery, vein or lymphatic vessel? Curr. Opin. Genet. Dev., 14: 499-505, 2004.

He, Y., de Castro, L. F., Shin, M. H., Dubois, W., Yang, H. H., Jiang, S., Mishra, P. J., Ren, L., Gou, H., Lal, A., Khanna, C., Merlino, G., Lee, M., Robey, P. G., and Huang, J. p53 loss increases the osteogenic differentiation of BMSCs. Stem Cells, 33: 1304-1319, 2015.

Ho, N., Gendron, R. L., Grozinger, K., Whelan, M. A., Hicks, E. A., Tennakoon, B., Gardiner, D., Good, W. V., and Paradis, H. Tubedown regulation of retinal endothelial permeability signaling pathways. Biology Open, 4: 970-979, 2015.

Hua, K. T., Tan, C. T., Johansson, G., Lee, J. M., Yang, P. W., Lu, H. Y., Chen, C. K., et al. N-α-acetyltransferase 10 protein suppresses cancer cell metastasis by binding PIX proteins inhibiting Cdc42/Rac1 activity. Cancer Cell, 19: 218-231, 2011.

Jacks, T., Remington, L., Williams, B. O., Schmitt, E. M., Halachmi, S., Bronson, R. T., and Weinberg R. A. Tumor spectrum analysis in *p53*-mutant mice. Current Biology, 4: 1-7, 1994.

Kalvik, T. V., and Arnesen, T. Protein N-terminal acetyltransferases in cancer. Oncogene, 32: 269-276, 2013.

Kang, J., Chun, Y. S., Huh, J., and Park, J. W. FIH permits NAA10 to catalyze the oxygen-dependent lysyl-acetylation of HIF-1α. Redox. Biol., 19: 364-374, 2018.

Khanh, V. C., Zulkifli, A. F., Tokunaga, C., Yamashita, T., Hiramatsu, Y., and Ohneda, O. Aging impairs beige adipocyte differentiation of mesenchymal stem cells via the reduced expression of Sirtuin 1. Biochem. Biophys. Res. Commun., 500: 682-690, 2018.

Kim, K. S., and Park, Y. Ewing sarcoma: a chronicle of molecular pathogenesis. Hum. Pathol., 55: 91-100, 2016.

Kisanuki, Y. Y., Hammer, R. E., Miyazaki, J., Williams, S. C., Richardson, J. A., Yanagisawa, M. Tie2-Cre transgenic mice: A new model for endothelial cell-lineage analysis *in vivo*. Dev. Biol., 15: 230-242, 2001.

Komori, T. Cell death in chondrocytes, osetoblasts, and osteocytes. Int. J. Mol. Sci., 17: 1-17, 2016.

Kuo, H. P., Lee, D. F., Chen, C. T., Liu, M., Chou, C. K., Lee, H. J, et al. ARD1 stabilization of TSC2 suppresses tumorigenesis through the mTOR signaling pathway. Sci Signal, 3: 2010.

Levy, A. D., Shaw, J. C., and Sobin, L. H. Secondary tumors and tumorlike lesions of the peritoneal cavity: Imaging features with pathologic correlation. RadioGraphics, 29: 347-373, 2009.

Lin, P. P., Wang, Y., and Lozano, G. Mesenchymal stem cells and the origin of Ewing's sarcoma. Sarcoma, 2011: 1-8, 2010.

Liszczak, G., Goldberg, J. M., Foyn, H., Petersson, E. J., Arnesen, T., and Marmorstein, R. Molecular basis for amino-terminal acetylation by the heterodimeric NatA complex. Nat. Struct. Mol. Biol., 20: 1098-1105, 2013.

Liu, H., Li, B. p53 control of bone remodeling. J Cell Biochem.,111(3): 529-534, 2010.

Magin, R. S., March, Z. M., and Marmorstein, R. The N-terminal acetyltransferase Naa10/ARD1 does not acetylate lysine residues. J. Biol. Chem., 291: 5270-5277, 2016.

Martin, D. T., Gendron, R. L,, Jarzembowski, J. A., Perry, A., Collins, M. H., Pushpanathan, C., Miskiewicz, E., Castle, V. P., and Paradis, H. Tubedown expression correlates with the differentiation status and aggressiveness of neuroblastic tumors. Clin. Cancer Res., 13: 1-8, 2007.

Meek, D. W. Regulation of the p53 response and its relationship to cancer. Biochem. J., 469: 325-346, 2015.

Myklebust, L. M., Damme, P. V., Stove, S. I., Dorfel, M. J., Abboud, A., Kalvik, T. V., Grauffel, C., Jonckheere, V., Wu, Y., Swensen, J., Kaasa, H., Liszczak, G., Marmorstein, R., Reuter, N., Lyon, G. J., Gevaert, K., and Arnesen, T. Biochemical and cellular analysis of Ogden syndrome reveals downstream Nt-acetylation defects. Hum. Mol. Gen., 24: 1956-1976, 2015.

Nostrand, J. L. V., Bowen, M. E., Vogel, H., Barna, M., and Attardi, L. D. The p53 family members have distinct roles during mammalian embryonic development. Cell Death Differ., 24: 575-579, 2017.

Palumbo, J. S., and Zwerdling, T. Soft tissue sarcomas of infancy. Semin. Perinatol., 23: 299-309, 1999.

Paradis, H., Liu, C.Y., Saika, S., Azhar, M., Doetschman, T., Good, W.V., Nayak, R., Laver, N., Kao, C.W., Kao, W.W., Gendron, R.L. Tubedown-1 in remodeling of the developing vitreal vasculature in vivo and regulation of capillary outgrowth in vitro. Dev Biol., 249:140-55, 2002.

Pishas, K. I., and Lessnick, S. L. Recent advances in targeted therapy for Ewing sarcoma. F1000Research, 5: 2-11, 2016.

Polonio-Vallon, T., Kirkpatrick, J., Krijgsveld, J., and Hofmann, T. G. Src kinase modulates the apoptotic p53 pathway by altering HIPK2 localization. Cell Cycle, 13: 115-125, 2014.

Reed, S. M., and Quelle, D. E. p53 acetylation: regulation and consequences. Cancers, 7: 30-69, 2015.

Rubio, R., Gutierrez-Aranda, I., Sáez-Castillo, A., Labarga, A., Rosu-Myles, M., Gonzalez-Garcia, S., Toribio, M. L., Menendez, P., and Rodriguez, R. The differentiation stage of p53-Rb-deficient bone marrow mesenchymal stem cells imposes the phenotype of *in vivo* sarcoma development. Oncogene, 32: 4970-4980, 2013.

Rufini, A., Tucci, P., Celardo, I., and Melino, G. Senescence and aging: the critical roles of p53. Oncogene, 32: 5129-5143, 2013.

Sato, T. N., Tozawa, Y., Deutsch, U., Wolburg-Buchholz, K., Fujiwara, Y., Gendron-Maguire, M., Gridley, T., Wolburg, H., Risau, W., and Qin, Y. Distinct roles of the receptor tyrosine kinases Tie-1 and Tie-2 in blood vessel formation. Nature, 376: 70-74, 1995.

Saunier, C., Støve, S. I., Popp, B., Gérard, B., Blenski, M., AhMew, N., et al. Expanding the phenotype associated with NAA10-related N-terminal acetylation deficiency. Hum. Mut., 37: 755-764, 2016.

Staines, K. A., MacRae, V. E., and Farquharson, C. The importance of the SIBLING family of proteins on skeletal mineralisation and bone remodeling. J. Endocrinol., 214: 241-255, 2012.

Starheim, K. K., Gromyko, D., Velde, R., Varhaug, J. E., and Arnesen, T. Composition and biological significance of the human N^{α}-terminal acetyltransferases. BMC Proceedings, 3: 1-12, 2009.

Sugiura, N., Adams, S. M., and Corriveau, R. A. An evolutionarily conserved N-terminal acetyltransferase complex associated with neuronal development. J. Biol. Chem., 278: 40113-40120, 2003.

Takiar, V., Ip, C. K. M., Mills, G. B., and Cheung, L. W. T. Neomorphic mutations create therapeutic challenges in cancer. Oncogene: 1-12, 2016.

Tang, Y., Zhao, W., Chen, Y., Zhao, Y., and Gu, W. Acetylation is indispensable for p53 acetylation. Cell, 133: 612-626, 2008.

Vo, T. T. L., Jeong, C., Lee, S., Kim, K., Ha, E., and Seo, J. H. Versatility of ARD1/NAA10-mediated protein lysine acetylation. Exp. Mol. Med. 50: 1-13, 2018.

Wall, D. S., Gendron, R. L., Good, W. V., Miskiewicz, E., Woodland, M., Leblanc, K., and Paradis, H. Conditional knockdown of Tubedown-1 in endothelial cells leads to neovascular retinopathy. IOVS, 45: 3704-3712, 2004.

Watroba, M., and Szukiewicz, D. The role of sirtuins in aging and age-related diseases. Adv. Med. Sci., 61: 52-62, 2016.

West, D. C. Ewing sarcoma family of tumors. Curr, Opin, Oncol., 12: 323-329, 2000.

Yoon, H., Kim, H., Chun, Y., Shin, D. H., Lee, K., Shin, C. S., Lee, D. Y., Kim, H., Lee, Z. H., Ryoo, H., Lee, M., Oh, G. T., and Park, J. NAA10 controls osteoblast differentiation and bone formation as a feedback regulator of Runx2. Nat. Commun., 5:5176: 1-14, 2014.

Yu, M., Gong, J., Ma, M., Yang, H., Lai, J., Wu, H., Li, L., Li, L., and Tan, D. Immunohistochemical analysis of human arrest-defective-1 expressed in cancers *in vivo*. Oncol. Rep., 21: 909-915, 2009. Dev. Biol., 230: 230-242, 2001.

Yu, H., Ge, Y., Guo, L., and Huang, L. Potential approaches to the treatment of Ewing's sarcoma. Oncotarget, 8: 5523-5539, 2017.